Catalytic strategies for improving specific fuel properties

Phuong T. M. Do, Steven Crossley, Malee Santikunaporn and Daniel E. Resasco*

DOI: 10.1039/b602366p

1. Introduction

As governments are urged to become more diligent in tackling environmental issues, legislatures in many countries continue to set increasingly stringent environmental standards on petroleum fuels, especially in reference to sulfur and polynuclear aromatic hydrocarbon (PAH or PNA) contents, which in turn, have a strong impact on NO_x and particulate matter (PM) emissions. Aromatics, especially polycyclic aromatics, produce PM or soot in jet, diesel, and gasoline engines.[1] At the same time, tests carried out on turbocharged and after-cooled heavy-duty direct injection engines show that increasing aromatics in diesel fuel also increases NO_x emissions.[2] In jet fuels, the high tendency of aromatics to form soot is described in terms of the smoke point, which becomes very low as the aromatics concentration increases. In diesel fuel, the presence of PAHs lowers the cetane number (CN), which determines the ignition quality of a fuel.[3] The 2005 European Union specifications for diesel stipulate a maximum content of polyaromatics of 11 wt% and a minimum cetane number of 51; for gasoline, the content of total aromatics cannot exceed 35 vol%.[4] Likewise, in the US the Environmental Protection Agency (EPA) might set in for the near future, a minimum CN of 40 and a maximum content for aromatics of 35% as standards for non-road, locomotive and marine diesel fuel. The EPA has already set an upper limit for sulfur content in diesel fuel of 15 ppm.[5] In California, the total aromatic content in diesel fuels allowed is 10 wt% maximum.

In the case of diesel fuel, an important property that defines the fuel quality is the cetane number (CN). Fuels with low-CN have poor ignition quality (*i.e.* knocking, noise, PM emissions) and make starting the engine difficult on cold days.[6,7] It is well known that CN is lowest for PAHs and highest for *n*-paraffins.[8,9] In normal paraffins, CN increases with the number of carbon atoms in the molecule. For naphthenic compounds and iso-paraffins the CN falls between those of aromatics and *n*-paraffins. In iso-paraffins, the CN decreases as the degree of branching increases.[10]

Fig. 1 shows the variation of CN in going from naphthalene to *n*-decane. Naphthalene, which has an extremely low CN, is a common aromatic compound in the diesel range. Converting it to paraffins would result in an increase in both blending and individual CN. Additionally, there would be a net gain in volume of fuel.[11] However, as discussed in this chapter, such a conversion path is not obvious, or even possible at high selectivities. It is clearly seen that, in order to convert naphthalene into high-CN molecules, a complete hydrogenation is required prior to selective ring opening (SRO), and more importantly, to obtain a straight-carbon-chain paraffin, the SRO should only occur at the substituted carbon centers.[12]

It must be noted that improving CN and meeting environmental regulations would require an excess demand for hydrogen; the issue of hydrogen balance opens a wide range of potential strategic decisions that the refiners must make; however, this

School of Chemical, Biological, and Materials Engineering, The University of Oklahoma, Norman, OK 73019, USA. E-mail: resasco@ou.edu; Tel: (405) 325-4370

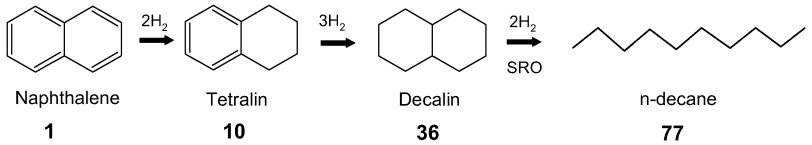

Fig. 1 Gradual improvement in cetane number of naphthalene caused by hydrogenation and subsequent selective ring opening. Adapted from ref. 12.

issue is not discussed in detail in this review. Possible solutions that refiners will consider may involve the partial oxidation of hydrocarbons, naphtha reforming, steam reforming of light hydrocarbons, and improved recovery and purification technologies.[13] The focus of this review is not on the sources of this hydrogen, but rather the catalytic routes that may be taken to meet the current an upcoming environmental regulations.

In a similar fashion, octane number (ON) is a key parameter in determining the quality of gasoline. High ON means high resistance of the fuel against knocking. In a combustion engine, a compressed mixture of fuel and air is introduced. Due to the thermal stability of each molecule and the ensuing radicals, some molecules tend to burn sooner than others, which causes knocking.[14] There are two types of octane number tests: research octane number (RON) and motor octane number (MON). RON typically provides an indication of how the fuel will perform under mild driving conditions, while MON represents more severe conditions. (RON + MON)/2 is the current ON that is reported at the pump. These values are based on a scale on which isooctane is 100 (minimal knock) and heptane is 0 (bad knock). In general, aromatics (*i.e.* benzene, toluene, *etc.*) and iso-paraffins have high ONs.[15] For iso-paraffins, branching is desirable, because it increases ONs, which is in contrast to CN. Therefore, *n*-paraffins are undesirable in gasoline, while they are desirable in diesel. To achieve the goal of making gasoline more environmentally friendly, while keeping its ON high, aromatics need to be converted to iso-paraffins with substantially higher ON.

Aromatics are typically included in gasolines to increase octane number. However, high aromatic content increases engine-out hydrocarbons and NO_x emissions.[16] Moreover, aromatics are the main precursors of exhaust benzene, a known carcinogenic, *via* dealkylation of substituted aromatics.[17] Therefore, reduction of total aromatic content, together with olefin content, is an important part of California phase III reformulated gasoline specifications,[18] with respect to the current allowed concentrations of benzene and total aromatics of 0.8 and 25 percent of volume, respectively.

In addition to CN and ON, the smoke point (SP), which is the maximum smoke-free laminar diffusion flame height, has been employed widely to evaluate the tendency of different fuels to form soot. This tool was first applied to kerosenes, later diesel, and then jet engine fuels.[19,20] Researchers have tried to relate smoke points of pure compounds to their molecular structure. It was found that the inverse of smoke point, which measures the potential of a fuel to form soot, increases from *n*-paraffins to iso-paraffins to alkylbenzenes to naphthalenes.[21,22] Since smoke points vary with experimental conditions, the concept of a threshold soot index (TSI), which is calculated from the smoke point, molecular weight, and experimental constants, has been used to compare the soot-formation tendencies of different fuel molecules.[23]

As stated above, molecular structures of hydrocarbon compounds greatly affect the different properties for fuels of different engines (*e.g.* combustion, self-ignition, homogeneous charge compression ignition engines).[24] For instance, fuels used in a diesel engine require long-chain paraffins to obtain high CN. Meanwhile, branching iso-paraffins are desirable for a gasoline engine. Therefore, in the present review, we describe the various tools available to first estimate CN, ON and TSI values of

individual hydrocarbons and then decide how the predicted values can be used in choosing the appropriate catalytic strategies (*i.e.* guided reaction pathways) that one can follow in order to maximize these properties.

In each of the pathways that we have considered in this review, it is assumed that an initial hydrogenation of the aromatics has been conducted and that the sulfur content is low enough as to avoid poisoning of the noble metals used in the different cases. Sulfide bimetallic catalysts are known to be very active in hydrogenation reactions. Phenanthrene, naphthalene, and tetralin are commonly employed as probe molecules for hydrogenation reactions. Since sulfides have relatively low activity, full hydrogenation cannot be achieved with these catalysts since at high temperatures equilibrium limitations appear. As a result, a second process of aromatic saturation catalyzed by noble metals is often considered.[25] Following saturation, the resulting naphthenic rings can be further converted *via* ring contraction (RC) and selective ring opening (SRO) reactions.

In the RC step, a 6-membered ring is isomerized over an acid catalyst or a bifunctional catalyst to a 5-membered ring, which subsequently can be opened selectively on a noble metal catalyst with high hydrogenolysis activity. Researchers have reported ring contraction reaction studies involving two-ring naphthenes, *i.e.* decalin. Ring contraction catalysts are typically zeolites and Pt-modified zeolites. For SRO reactions, iridium-based catalysts often stand out as the most active. They are used in the ring opening reactions of alkylcyclohexanes and alkylcyclopentanes. Ring opening at different C–C bond positions also has a great impact on the properties of the resulting products, such as CN and ON.

2. Prediction of fuel properties

2.1 Importance of fuel property predictions

One of the important tasks in the improvement of diesel fuels is the increase in cetane number (CN). There are several possible routes for increasing CN of a diesel fuel, including blending with Fischer-Tropsch (FT) fuels or adding cetane boosters.[26,27] However, these routes have their limitations; the problem of blending FT products is the high cost of this fuel,[28] the problem of cetane boosters is their low stability and very high flammability, causing the entire fuel to become more dangerous.[27] A third option is to modify, *via* a combination of aromatic saturation and selective ring opening, the structure of the molecules present in the fuel. Ring opening products (ROP) resulting from each of the possible RO pathways have different CNs. Therefore, in order to determine if a particular ring opening reaction has a positive impact on the CN of a diesel fuel, the chemistry behind the individual reactions must be understood. For this reason, a number of model molecules, typically found in diesel fuel, were chosen to analyze the effect of the possible RO paths on their CN. The same methodology can be applied to ON and TSI. Although lists of CN, ON and TSI of individual compounds are available, there are still many molecules potentially produced from chemical reactions of model feeds which do not have these properties measured. For this reason, prediction tools are needed to compute those important fuel properties based on molecular structure and other known physical parameters. While a wide variety of techniques have been used to estimate various fuel properties, the techniques used here all involve correlations between the structure of the molecules and the properties themselves. These techniques will be discussed in the following section.

2.2 Methods for property predictions

Classical chemo metric methods, such as the Quantitative Structure Activity Relationships, QSAR, can be used to relate the chemical characteristics of a molecule to its structure. QSAR methods have been widely used in the pharmaceutical field for drug design, but they are also very useful for many other

applications.[29,30] In the context of fuel properties, QSAR methods can be used for prediction of CN, ON and TSI. We have obtained fuel property predictions with MDL® QSAR (version 2.2.0.0.446 (SP1) from MDL Information Systems, Inc.) software that has the ability to calculate over 400 *molecular descriptors* of a particular molecule, which can then be used to predict a fuel property. These molecular descriptors can be based on the size, shape, charge, *etc*. of the molecule. Although it is not straightforward to extract direct physical information regarding combustion properties from each of these descriptors, they can be used as effective inputs for statistical models that allow us to predict the desired parameters. In order to determine the best possible descriptors to use in a model, a genetic algorithm is used in order to lower the number of descriptors down to a computationally reasonable number (<50); multiple regressions are then performed with all possible descriptor combinations in order to determine the best combination for a specified number of variables. The numerous predictions for a fuel property from each model with varying numbers of variables are then compared with an external set of data that is not included in the fitting in order to determine the overall best method.

2.2.1 Prediction of cetane number. Predictions of CN have been made by several authors using a variety of different types of inputs including ^{13}C NMR, IR spectra, refractive index, parameter lumps, GC analysis, and multiple other types of properties.[31,32] In 1995, Ladommatos *et al*.[32] introduced twenty-two equations to predict the CN of diesel fuel. The predictive capability of some equations was high (standard error of CN < 2). He also reported that it is unlikely that the standard error can be reduced significantly below 1.5, because the measured cetane numbers are themselves subject to experimental error. However, more than ten years later, Ghosh *et al*.[33] reported an improvement in CN prediction with standard error of only 1.25. A simple composition-based model is used to correlate CN of diesel fuels with a total of 129 various hydrocarbon lumps determined by a group of supercritical fluid chromatography, gas chromatography, and mass spectroscopic methods.

These models allow us to estimate the CN of diesel fuel mixtures. However, to evaluate the impact of specific reactions on specific molecules, the cetane values of individual compounds are needed. For this purpose, molecular descriptors were used in order to predict the CNs of individual hydrocarbons. The quality of the model is represented by Fig. 2a and b. Fig. 2a shows a plot of the CN values calculated from the model *versus* the actual measured CN inputs. This plot is important to ensure that the errors in prediction do not deviate significantly to one side or the other in a systematic way. As the number of molecular descriptors used in the model increases, the error between the calculated and measured values in the model continuously decreases. To prevent an over-fitting of the data a maximum number of descriptors is recommended. One can clearly see in Fig. 2b that, as the number of descriptors increases, the root mean squared (RMS) error in the model continuously decreases, while the error in an external set of data reaches a minimum and then increases again as over-fitting starts to occur. The external data set is composed of nine data points that represent the entire range of data. The reason for the smaller degree of error in the external dataset than in the model is that the external dataset consisted only of Ignition Quality Tester (IQT™) derived CNs from one particular machine. The database used to feed the model[34] was composed of both, engine test CNs and IQT measurements from various sources. The large variety of sources causes a relatively high error in the database itself, so if possible a single database source should be used.

Compared with the artificial neural network (ANN) approach used in previous work to predict CN[12] the linear regression model by QSAR is as good or better and easier to implement. The predicted CN values, some of which are tabulated in Table 1, will be employed below to evaluate the different catalytic strategies to optimize the fuel.

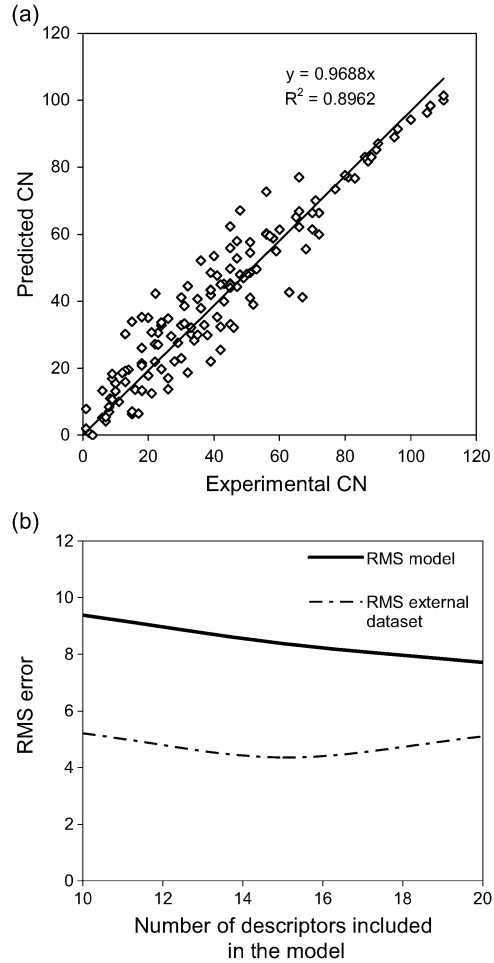

Fig. 2 (a) Calculated *versus* observed CNs. The error is well dispersed, and does not deviate much from the ideal slope of 1. (b) Comparison between the Root Mean Squared errors of the calculated values and the number of descriptors included in the CN model.

2.2.2 Prediction of octane number. Similar to the case of CN predictions, the majority of the work reported in the literature has focused on the prediction of ON of gasoline mixtures.[35,36] For example, in the 1970s, Anderson, *et al.*[37] constructed a method to estimate the RON of different gasolines by using the results from gas chromatography. This model had a standard error of 2.8 points, probably due to the assumption of linearity in octane blending. Deviations due to nonlinear interactions among different hydrocarbon groups (*i.e.* paraffins, olefins, aromatics, *etc.*) can be significant.[38] In order to estimate the ON of a mixture of hydrocarbons, interactions between the molecules involved must be considered. It has been reported that hydrocarbons belonging to the same molecular class blend linearly; *i.e.*, paraffins blend linearly with other paraffins, olefins blend linearly with other olefins, and so on. However, a blend of paraffins and olefins may exhibit significant deviations from linearity. A diagram that helps to illustrate this concept is shown in Fig. 3.[14] Curve a displays a positive interaction or equivalently a positive deviation from linearity, curve c displays a negative interaction, and curve b displays no interaction.

For a mixture containing more than two compounds, this system becomes even more complicated. Very recently, Ghosh *et al.*[14,33] have created an improved model

Table 1 (a) Predicted fuel property values for paraffins and cycloparaffins. (b) Predicted fuel property values for aromatics and olefins including the models used for the predictions

(a)

Paraffins	TSI	RON	MON	CN	Cycloparaffins	TSI	RON	MON	CN
n-Heptane	2	0	4	52	1,1,2-Trimethylcyclohexane	13	96	91	29
n-Hexane	1	29	33	45	1,1,2-Trimethylcyclopropane	9	105	88	13
2,2,3,3-Tetramethylhexane	15	116	95	26	1,1,*cis*-2, *trans*-4-Tetramethylcyclopentane	12	100	95	21
2,2,3,3-Tetramethylpentane	8	117	92	21	1,3-Dimethylcyclohexane	7	65	64	31
2,2,3-Trimethylbutane	8	113	103	9	1,*cis*-2,*trans*-3-Trimethylcyclohexane	8	84	83	30
2,2,3-Trimethylpentane	9	106	100	14	1,*cis*-2-Dimethylcyclohexane	8	77	76	30
2,2,4-Trimethylpentane	5	96	97	21	1,*cis*-2-Dimethylcyclopropane	4	109	89	17
2,2-Dimethylbutane	8	89	96	23	1,*cis*-3,*trans*-5-Trimethylcyclohexane	6	70	66	23
2,2-Dimethylheptane	9	52	54	49	1,*cis*-3-Dimethylcyclohexane	7	65	64	31
2,2-Dimethylhexane	8	74	80	40	1,*cis*-3-Dimethylcyclopentane	6	76	73	27
2,2-Dimethyloctane	9	49	46	55	1,*cis*-4-Dimethylcyclohexane	7	71	66	23
2,2-Dimethylpentane	7	89	89	30	1,*trans*-2,*trans*-4-Trimethylcyclohexane	7	77	74	28
2,3,3-Trimethylpentane	9	111	102	17	1,*trans*-2-Dimethylcyclohexane	8	77	75	29
2,3-Dimethylpentane	3	88	83	20	1,*trans*-2-Dimethylcyclopropane	4	107	86	14
2,4-Dimethylhexane	2	62	67	29	1,*trans*-3-Dimethylcyclohexane	7	72	66	24
2,4-Dimethylpentane	1	88	83	28	1,*trans*-4-Dimethylcyclohexane	7	63	64	32
2-Methyl-3-ethylpentane	4	81	79	12	1-Methyl-1-ethylcyclohexane	14	67	76	39
2-Methylheptane	3	19	29	46	1-Methyl-*cis*-2-*n*-propylcyclohexane	7	25	37	38
2-Methylpentane	2	75	77	29	1-Methyl-*trans*-2-*n*-propylcyclohexane	7	26	36	36
3,3-Diethylpentane	12	83	97	17	3-Cyclohexylhexane	7	16	43	38
3,4-Dimethylhexane	4	71	73	20	Cyclopentane	5	98	79	26
3-Methylheptane	4	27	35	37	Cyclopentylcyclopentane	15	14	12	52
3-Methylhexane	3	57	59	27	Cyclopropane	5	149	125	5
3-Methylpentane	3	80	78	23	isopropylcyclohexane	9	64	60	35
4,5-Diethyloctane	7	0	25	18	Methylcyclohexane	7	70	70	30
Isononane	4	7	11	39	Methylcyclopentane	7	80	74	24
Isopentane	2	96	93	21	*tert*-Butylcyclohexane	14	96	85	31

(b)

Aromatics	TSI	RON	MON	CN	Olefins	TSI	RON	MON	CN
1,2,3-Trimethylbenzene	57	108	98	8	1-Pentene	6	89	76	14
1,2,4-Trimethylbenzene	54	110	102	5	2,2-Dimethyl-*trans*-3-hexene	12	109	93	12
1,2-Diethyl-3-methylbenzene	59	106	97	6	2,3,3-Trimethyl-1-butene	29	108	91	7
1,2-Dimethylbenzene	54	109	99	11	2,3,3-Trimethyl-1-pentene	31	105	90	16
1,3-Diethylbenzene	55	113	99	4	2,3-Dimethyl-1-butene	17	102	85	13
1,3-Dimethylbenzene	49	115	106	2	2,3-Dimethyl-1-pentene	17	98	83	18
1,4-Diethylbenzene	58	109	94	0	2,3-Dimethyl-2-hexene	16	93	80	24
1.2.3.5-Tetramethylbenzene	56	109	102	6	2,5-Dimethyl-2,4-hexadiene	11	92	76	21
1-Methyl-2-allylbenzene	68	92	81	9	2,5-Dimethyl-2-hexene	6	95	81	27
1-Methyl-3-ethylbenzene	54	113	102	5	2-Methyl-1-hexene	8	86	76	39
1-Methyl-3-*n*-propylbenzene	48	110	96	12	2-Methyl-*trans*-3-heptene	7	90	79	26
1-Methyl-4-ethylbenzene	55	114	102	2	2-Methyl-*trans*-3-hexene	6	99	86	16
Allylbenzene	63	106	93	3	3,4-Dimethyl-*cis*-2-pentene	12	101	85	0
Ethylbenzene	53	112	99	7	3-Methyl-*trans*-2-hexene	5	90	77	10
Isopropyl benzene (CUMENE)	59	112	102	6	3-Methyl-*trans*-2-pentene	6	97	82	6
Mesitylene	48	119	111	−7	4-Methyl-1-hexene	9	86	74	19
ortho-Xylene	54	109	99	10	4-Methyl-1-pentene	9	93	76	20
sec-Pentylbenzene	57	97	89	16	4-Methyl-*trans*-2-hexene	7	94	84	7
Styrene	67	107	94	0	4-Methyl-*trans*-2-pentene	5	98	85	10
tert-Butylbenzene	68	112	107	2	5-Methyl-*trans*-2-hexene	4	90	78	18
Toluene	49	111	101	4	*trans*-3-Hexene	4	92	82	11

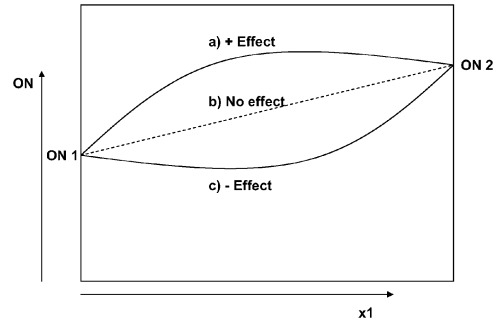

Fig. 3 Deviations from non-linear mixing of pure component ON's of a binary mixture. Adapted from ref. 14.

from experimental RON and MON data of 1471 gasoline fuels. GC analysis was conducted in order to determine the compositions of each fuel; then, molecular lumps were generated and correlated to the RON and MON of the mixtures. Blending parameters were correlated to RON and MON by creating a constrained least-squared minimization problem and utilizing a Levenberg-Marquadt algorithm. Interaction parameters were obtained between large groups of molecules (*i.e.* between paraffins and olefins, *etc.*) in order to minimize the number of calculations. This molecular lumping technique proved to be quite accurate, with a standard error of $\sim$1 for prediction of both RON and MON of fuel mixtures. The equation developed can be readily applied as follows:

$$\mathrm{ON} = \frac{\sum\limits_{\mathrm{PONA}} v_i\beta_i\mathrm{ON}_i + \left(\frac{k_{\mathrm{PN}}^{(a)}v_n + k_{\mathrm{PO}}^{(a)}v_{\mathrm{O}}}{1 + k_{\mathrm{PN}}^{(b)} + k_{\mathrm{PO}}^{(b)}v_{\mathrm{O}}}\right)\sum\limits_{\mathrm{P}} v_i\beta_i\mathrm{ON}_i}{\sum\limits_{\mathrm{PONA}} v_i\beta_i + \left(\frac{k_{\mathrm{PN}}^{(a)}v_n + k_{\mathrm{PO}}^{(a)}v_{\mathrm{O}}}{1 + k_{\mathrm{PN}}^{(b)} + k_{\mathrm{PO}}^{(b)}v_{\mathrm{O}}}\right)\left(\sum\limits_{\mathrm{P}} v_i\beta_i - \sum\limits_{\mathrm{P}} v_i\right)} \quad (1)$$

In this equation, all molecules are divided into four groups: paraffins (P), olefins (O), naphthenics (N), and aromatics (A). The v_i values represent the volume fractions of each component used, while the β_i values are the blending values, which were calculated for each of the molecular lumps shown in Table 2. Pure component octane numbers used are designated as ON_i, but one should note that in the development of the model, 57 molecular lumps were made based on GC analysis, and pure component ONs were assigned to each lump, and not necessarily each pure component. The k_i values are calculated interaction parameters between paraffins, olefins, and naphthenics, and are also shown in Table 2. Based on this equation, and knowing the composition and pure octane numbers of a fuel mixture, an estimation of the blending ON may then be made.

Table 2 Parameter values for eqn (1); adapted from ref. 14

Molecular class	Molecular lumps	β(RON)	β(MON)
n-Paraffins	$n\mathrm{C_4}$–$n\mathrm{C_{12}}$	2.0559	0.3092
Iso-paraffins	$\mathrm{C_4}$–$\mathrm{C_{12}}$ mono-, di-, and trimethyl-iso-paraffins	2.0204	0.4278
Naphthenes	$\mathrm{C_5}$–$\mathrm{C_9}$ naphthenes	1.6870	0.2821
Aromatics	Benzene-$\mathrm{C_{12}}$ aromatics	3.3984	0.4773
Olefins/cycloolefins	$\mathrm{C_4}$–$\mathrm{C_{12}}$ linear, branched, and cyclic olefins	8.9390	10.0000
Oxygenates	MTBE, EtOH, TAME	3.9743	2.0727
Interaction parameters	$k_{\mathrm{PN}}^{(a)}$, $k_{\mathrm{PN}}^{(b)}$, $k_{\mathrm{PO}}^{(a)}$, $k_{\mathrm{PO}}^{(b)}$	0.2,2.4,0.4,3.6	0.2,2.4,0.4,3.6

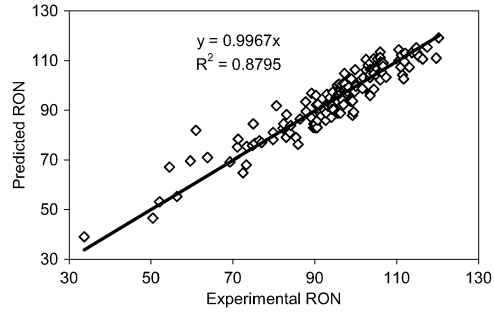

Fig. 4 The predicted *versus* observed RON values for olefins and aromatics. The model used 22 descriptors.

In addition to the ONs of gasoline mixtures, ONs of individual compounds are needed when the effect of specific catalytic strategies is to be assessed. As previously described, instead of the artificial neural network used in previous studies, linear regression models were used in this case for the sake of simplicity and repeatability, at the expense of a small increase in error. Fig. 4 shows the predicted *versus* the observed RON values for olefins and aromatics, which had a RMS error of 4.8 points. MON predictions for olefins and aromatics also showed a RMS error of 5.8 points. Separate models were constructed for the group of *n*-paraffins, iso-paraffins, and cyloparaffins in order to get a better fit of data for the extreme low and high ON molecules. The RON and MON predictions for *n*-paraffins, iso-paraffins, and naphthenes have RMS errors of 8.7 and 6.8, respectively. Predicted values of ON for different compounds are also shown in Table 1. It is important to mention that the ON predictions result in larger errors in the regions of lower ON due to the smaller number of measured data points used in this region for the development of the models. In industrial practice, this region is less important because the amounts of compounds with ON's lower than 40 are very low, and will not contribute much to the total ON of the fuel. For fundamental studies, however, it is often important to be able to estimate the ON's of these compounds because they may be present in large amounts for a given chemical reaction. It is still very important to realize that ON values that are in the very low ON range or those that may be extrapolated to negative numbers may not be very accurate. The trends, however, are still captured by the model and can be very useful in determining how beneficial a particular reaction is in the overall reaction scheme.

2.2.3 Prediction of threshold soot index (TSI). Recent studies have been devoted to the prediction of the TSI of various individual hydrocarbons,[39] using the database compiled by Olson *et al*.[20] However, the range involved in these predictions is rather limited, covering mostly the kerosene range as TSI is most relevant for this hydrocarbon range. The accuracy of the TSI values greatly diminishes at both extremes, high and low values, due to the nature of the experimental measurement. At very high smoke points, the values of TSI are very small because TSI is inversely related to the smoke point. Consequently, the hydrocarbons with high smoke points are all very close together on the TSI scale, so small deviations in TSI correspond to large deviations in smoke point. At the other end of the scale, very small smoke points produce large TSI values, with small deviations in the smoke point producing large deviations in the TSI. For these reasons, it is expected that TSI values are more accurate in the middle of the scale, where the instruments and the correlation are much more precise (see Fig. 5). The predicted threshold soot indices (TSI) of different hydrocarbon compounds are tabulated in Table 1, together with cetane and octane numbers.

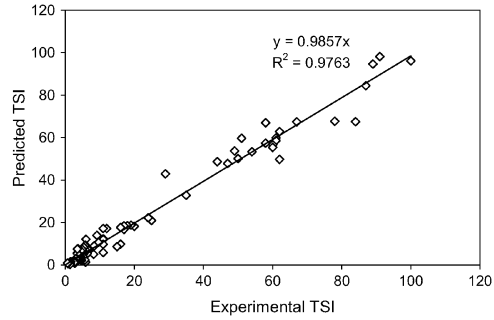

Fig. 5 The predicted *versus* experimental values for TSI.

2.2.4 Correlation between particulate matter (PM) emission and fuel properties. Besides the fact that these fuel properties must be at a certain minimum number in order to meet current EPA regulations, there are other important results that can be obtained from these fuel properties. As mentioned in the introduction, TSI provides an indication of how much PM a particular fuel will produce. The primary reason for the high CN regulations is the fact that the unburned hydrocarbons resulting from low CN fuels produce PM or soot, which is harmful to human health. As described above, CNs of individual compounds heavily depend on their molecular structures. For example, in an attempt to demonstrate the relationship between paraffinic molecular structure and soot formation in the high temperature range corresponding to the in-cylinder flame zone, Nakakita *et al.*[40] have carried out an investigation to measure the soot yields of isomeric hexanes in a shock tube. The temperature dependence of the yield of soot formation was found to follow a bell-shaped curve, with a maximum at about 2000 °C for all four isomers. These maximum yields are summarized in Fig. 6. It is seen that the soot production increases in the following order:

cyclohexane > 2,2-dimethylbutane > 2-methylhexane > *n*-hexane.

Similar to the soot formation in the high temperature range, PM precursor formation at intermediate temperatures is also influenced by the paraffinic molecular structure. It was proposed that the soot formation yield decreases in the order: cycloparaffin > 2-branched iso-paraffin > 1-branched iso-paraffin > normal

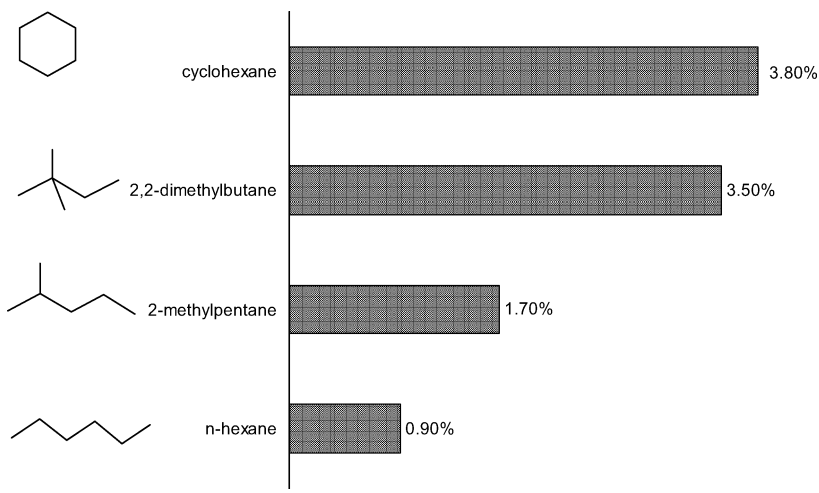

Fig. 6 Comparison of soot yield for various hexanes. Adapted from ref. 40.

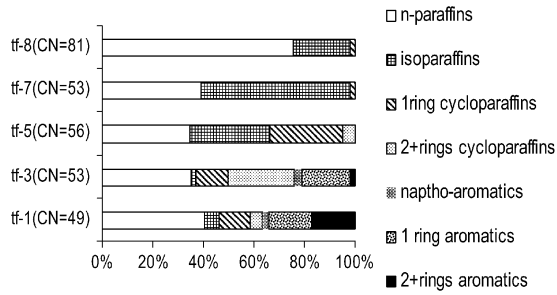

Fig. 7 Molecular composition of matrix fuels. Adapted from ref. 41.

paraffin. This trend is opposite to the cetane number trend, in which naphthenes have the lowest CNs and normal paraffins have the highest CNs.

One might be tempted to conclude that soot formation always decreases with increasing CN. However, Androulakis *et al.*[41] have clearly demonstrated that CN alone may be misleading. They conducted experiments with model feeds fed in a high-speed diesel engine with fuels of varying overall compositions, but practically the same CN. Compositions of the fuels investigated are summarized in Fig. 7. The first fuel is denoted as TF-1 and has a composition similar to current market diesel fuel, although with increased levels of two-ring aromatics. Except for TF-8, the CNs of all other fuels are in a similar range, but the compositions vary considerably. The PM emissions from the advanced high-speed direct injection (HSDI) diesel engines for different fuels were measured and the results are shown in Fig. 8. It was observed that, under high and medium load conditions (2800 rpm/60% and 2200 rpm/40% loads), PM emissions from TF-1 and TF-3, which contain more aromatics, were 60%–70% higher than those from the paraffinic fuels TF-5, TF-7, and TF-8. When comparing the PM emissions from TF-5 and TF-7, which have almost equivalent CNs, cycloparaffins (naphthenes) are seen to have a higher PM formation tendency than iso-paraffins or *n*-paraffins. As more aromatics and naphthenes are introduced, the amount of PM will increase, even while keeping the same CN, in good agreement with previous observations.[42] An exception was observed for TF-8 that contained the largest amount of *n*-paraffins. It does not yield the PM reductions that one may have expected. In fact, the very high CN of TF-8 (CN = 80.5) results in a significantly decreased ignition delay. Consequently, combustion is initiated before sufficient fuel-air mixing has occurred. This could be altered, however, by changing the engine parameters. The general trends identified from the study of PM emission HSDI diesel engines are: higher aromatics, naphthenes, CN, and density all lead to increased PM. These results increase the importance of utilizing other fuel properties

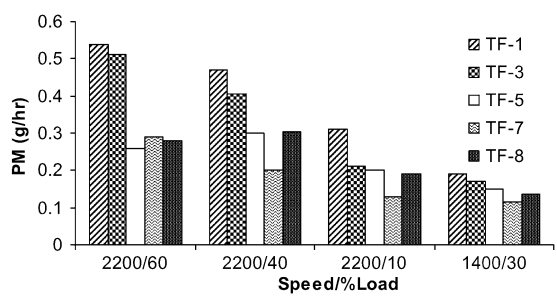

Fig. 8 Engine-out exhaust PM results from tests of several fuels at fixed speed/load conditions of an advanced, high-speed, direct injection diesel engine. Adapted from ref. 41.

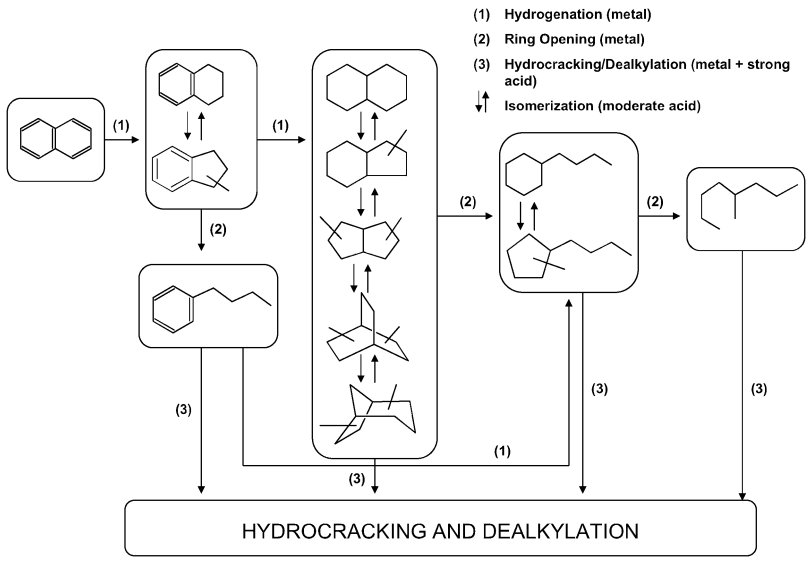

Fig. 9 Key reactions during the conversion of multiring aromatics to paraffins. Adapted from ref. 11.

in the design of a given fuel, such as TSI, that will provide a better indication of the fuel tendency to form PM than CN alone.

3. Catalytic strategies to optimize fuel properties

As shown above, CN and ON are important properties of diesel and gasoline fuels, respectively. Although a set of large databases are available, cetane and octane values of many individual compounds are still missing. Therefore, the prediction tools we have developed are very useful in correlating the molecular structures with properties of fuels. In this section, the predicted CN and ON values are implemented to construct the most effective catalytic strategies to optimize CN for diesel and ON for gasoline.

3.1 Improving cetane number

Fig. 1 shows that, as expected, fully-hydrogenated naphthalene (decalin) has a CN of 36, much higher than naphthalene, but still rather low compared to the expected requirements for diesel fuel. Therefore, further conversion *via* ring opening should be considered to generate paraffins and isoparaffins of higher-CN. As proposed by McVicker *et al.*,[11] decalin can undergo either ring opening or hydrocracking to alkane products (see Fig. 9). Ring opening reactions can occur by different pathways depending on the catalyst present; that is, *via* free radical reactions without a catalyst, *via* carbocation chemistry on acid catalysts, and *via* hydrogenolysis on metal catalysts. The free radical route, which follows thermal decomposition at high temperatures, produces low yield of selective ring opening products,[43] therefore, it will not be considered further. In this section, an analysis of acid-catalyzed and metal-catalyzed ring opening will be presented.

3.1.2 Acid-catalyzed ring opening of two-ring naphthenes. As proposed by Kubica *et al.*,[44,45] McVicker *et al.*,[11] and our own group,[46] on acid catalysts decalin first undergoes ring contraction (RC) and then ring opening (RO) reactions, as illustrated in Fig. 10. Six-membered rings can be activated on acids *via* formation of a

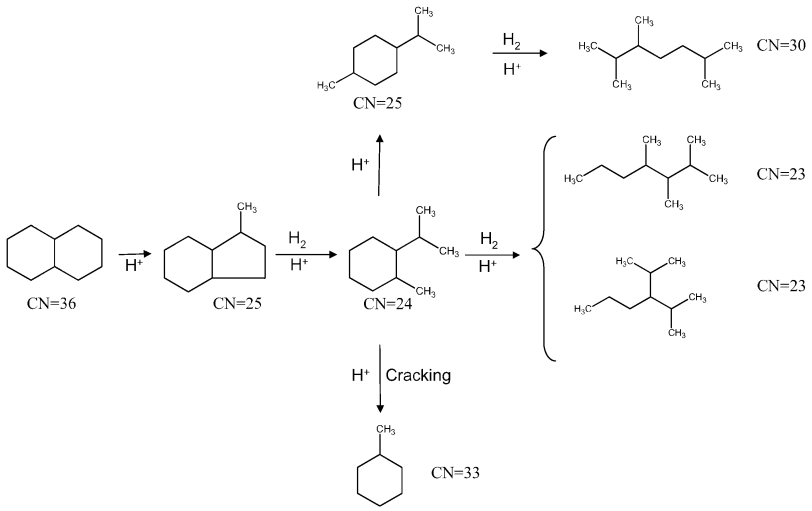

Fig. 10 Cetane number of intermediates and products of the reaction pathway of acid-catalyzed ring opening of decalin. Adapted from ref. 12.

carbocation, which can be generated by either protolytic cracking[47] or olefinic intermediates through hydrogen transfer. The main products of the RC reaction are alkyl-bicyclononanes and bicyclooctanes. A list of some of the most common RC products, along with their respective CNs, is included in Table 1.

As demonstrated by McVicker *et al.*,[11] ring opening of a 6-membered ring is more difficult than a 5-membered ring due to high ring strain of the later. Consequently, as conversion increases, the reaction proceeds from RC products to RO products resulting from the opening of a 5-membered ring *via* β-scission and hydrogenation of corresponding olefins. Additionally, additional products can be formed through methyl shift isomerization, which is a well-known mechanism in zeolite chemistry.[48] This transformation is included in the example of Fig. 10 (top path), in which the product of the first ring opening is further converted *via* methyl shift. The CN of other ring-opening products, alkylcyclohexanes and alklylcyclopentanes, are also included in Table 1. It is important to note here that some products from the ring opening of the first ring do not have significantly higher CN than the initial feed. As a result, opening of the second ring is needed to achieve higher CN. However, as illustrated on the right hand side of the scheme in Fig. 10, the opening of the second ring by itself is not a guarantee of high CN. For example, over an acidic catalyst that would open the second ring *via* a typical β-scission, this reaction would yield the type of highly branched isoparaffins shown in Fig. 10. The CN of the products from second ring-opening are also included in Table 1. Based on these values, it can be concluded that second ring-opening products obtained over an acidic catalyst may give rise to a few products with higher CN than the first ring-opening or the initial RC products, but most of them have similar or even lower CN than that of the feed. In addition, alkanes and side chains on naphthenic rings crack at 10–1000 faster rates than naphthenic rings on acid catalysts. This unavoidable cracking would result in a substantial loss of original molecular weight and a lower CN than the original feed.

3.1.2 Metal-catalyzed opening of C5 and C6 rings. Given the limitations of acid catalysts for improving CN, we have focused on the use of metal catalysts with high hydrogenolysis activity.[49] In this section, we have evaluated the possibility of using metal catalysts for the opening of the first and second rings. Noble metals such as

Rh, Ir, and Ru, are well known for being active hydrogenolysis catalysts.[50–53] They are particularly effective for opening five-member rings, but much less effective for opening six-member rings. For example, McVicker *et al.*[11] have shown that while alkylcyclopentanes can be readily ring-opened by low temperature hydrogenolysis over Ir, the corresponding ring opening of alkylcyclohexanes is almost a hundred times slower. They have proposed the addition of a mild acidity function to provide the catalyst the necessary ring-contraction activity without significant cracking. Therefore, we have evaluated the ring opening of both C6 and C5 rings under the assumption that they can occur after a RC step.

Hydrogenolysis of naphthenic rings on metals can proceed by different mechanisms. The most common hydrogenolysis mechanism that typically occurs on metals such as Ir and Rh is *via* the dicarbene intermediate. In this mechanism, the endocyclic C–C bond cleavage occurs on unsubstituted secondary C atoms. On Ir catalysts, this path was found to be independent of particle size and dispersion, but it is strongly dependent on the type of support used.[54] This insensitivity to particle size on Ir catalysts contrasts with the well known structure-sensitivity on Pt catalysts. For example, Gault *et al.*[55] studied the effect of metal particle size in Pt/Al_2O_3 catalysts for the ring opening of methylcylopentane and observed that on highly dispersed Pt/Al_2O_3, there was an equal chance of breaking any endocyclic C–C bond—a result that was attributed to a π-allyl mechanism that competes with the dicarbene mechanism. This mechanism derives from π-absorbed-olefins that require a flat adsorption of three neighboring carbon atoms interacting with a single metal site on the catalyst surface. On the other hand, on Pt catalysts with larger metal particles, secondary–secondary C–C bonds were preferentially broken, according to the dicarbene mechanism mentioned above. In this case, unlike the π-allyl mechanism, two endocyclic carbon atoms are involved with two adjacent metal atoms in the formation of the dicarbene intermediate, although the activity of Pt for this reaction path is much less than that of Ir.

To explain the observed rupture of sterically-hindered substituted tertiary–secondary C–C bond on these low dispersed Pt catalysts, a third mechanism was proposed that competes with the dicarbene mechanism.[55] This third mechanism involves a metallocyclobutane species as an intermediate. In fact, both McVicker *et al.*[11] and Coq *et al.*[56] have cited the metallocyclobutane mechanism as responsible for the observed hydrogenolysis of 1,2,4-trimethylcyclohexane and 2,2,3,3-tetramethylbutane, respectively.

We evaluate here the CN that would result when either the unsubstituted C–C (dicarbene) or substituted C–C bond cleavage occurs. First, when the dicarbene mechanism is dominant, a reaction path like the one shown in Fig. 11 can be expected. In this figure we have only considered C–C cleavage of unsubstituted atom pairs for direct opening of C6 rings or C5 rings produced by a previous RC reaction. An important conclusion that can be drawn from this analysis is that no substantial gain in CN can be achieved by RO *via* dicarbene mechanism. From Fig. 11 and Table 1, it can be seen that the CNs of the second-ring-opened products obtained *via* the dicarbene mechanism are just slightly better than those obtained *via* the acid catalyzed reactions. This limited improvement is because the breaking of the unsubstituted secondary–secondary C–C bond still leads to products with a high degree of branching. Not only are these molecules highly branched, but most branches are very short, in most cases just a methyl group. This is a disappointing result that weakens previous optimistic strategies, since the most active hydrogenolysis metal catalysts (Ir, Rh) operate primarily *via* the dicarbene mechanism.[11]

Conversely, if the ring opening could take place on a catalyst that favors the breaking of substituted tertiary–secondary C–C bonds and some of the even more sterically hindered tertiary–tertiary C–C bonds, a typical reaction path might follow the scheme of Fig. 12. The CNs of these products are considerably higher than the ones obtained *via* either acid catalyzed or dicarbene ring opening. Actually, the CNs of every one of the second ring opening products presented in Fig. 12 and Table 1 are

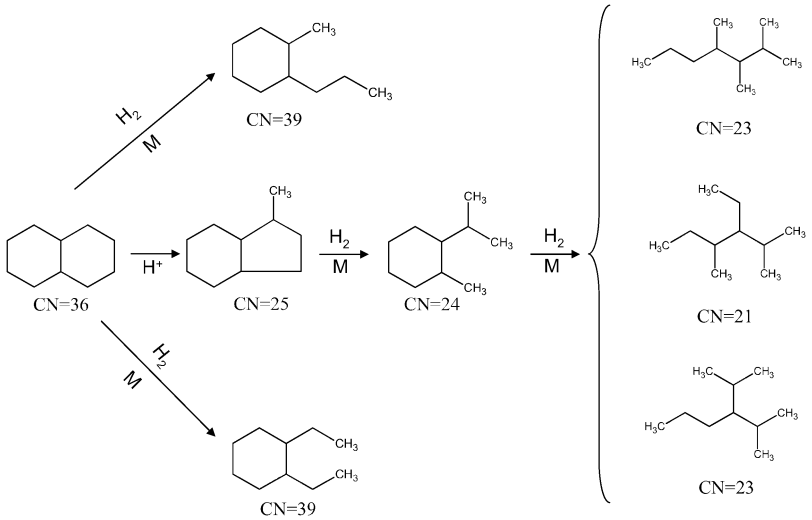

Fig. 11 Cetane number of intermediates and products of the reaction pathway of metal-catalyzed ring opening of decalin *via* dicarbene mechanism. Adapted from ref. 12.

greater than the CN of the decalin feed. From this analysis, it can be concluded that the only successful strategy to significantly increase the CN of decalin feedstocks should be based on a precisely tailored catalyst with high selectivity towards the cleavage of substituted C–C bonds. Our studies show that while Ir shows a very low selectivity to this path when supported on silica, an increased selectivity towards the cleavage of substituted bonds is observed when the support is alumina.

3.2 Improving octane number

For a long time, the content of aromatics in gasoline has been relatively high since they bear high ON.[35] However, they cause formation of PM during combustion and, if unburned, they are harmful to human health. Therefore, the current trends consider minimization of aromatics, which causes a significant loss in ON. It is of interest to investigate the pathways to convert aromatics into non-aromatic products that keep the same number of carbons and a high ON. As highlighted earlier, highly

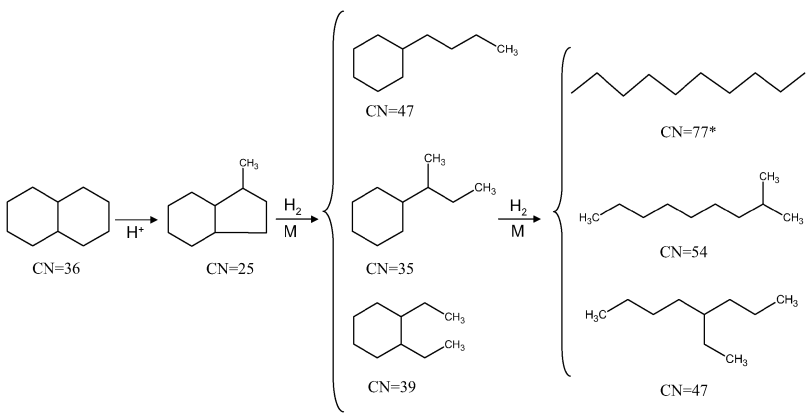

Fig. 12 Cetane number of intermediates and products of the reaction pathway of metal-catalyzed ring opening of decalin *via* substituted carbon center. Adapted from ref. 12.

branching isoparaffins have high ONs. In this section, we will analyze different reaction pathways to optimize the ON from an aromatic compound. The ON values predicted from the methods shown above will be used to find the preferred pathways, such as a silica-supported Ir catalyst.[49]

3.2.1 Acid-catalyzed ring contraction. Toluene is chosen here as a probe molecule because it is one of the typical aromatic compounds present in the gasoline range. It has a high RON of 119, but after saturation (*i.e.*, to methylcyclohexane (MCH)) this number drops to 73. Similar to the case of CN, we analyze the different reaction pathways on acid and metal catalysts following an initial hydrogenation (aromatic saturation) step. It is well known that dealkylation and isomerization (including ring contraction) commonly occur on an acid function.[57,58] Fig. 13 shows several direct reactions from MCH. In the top path, MCH undergoes demethylation to form cyclohexane (RON = 84), which is a gain of 11 points with respect to MCH, but when compared to the original toluene feed, dealkylation of MCH is not a good option. However, if MCH is isomerized to yield four ring contraction products (RC), three of these products (dimethylcyclopentanes) have relatively high octane numbers, with the exception of ethylcyclopentane (ECP). Highly branched 1,1-dimethylcyclopentane (1,1-DMCP) has the highest ON among them.

The chemical reaction pathways of MCH on acidic catalysts have been studied previously. Mignard *et al.*[59] investigated the reaction of MCH on Pt/USY. Their results indicated that MCH undergoes a ring contraction (RC) step to form dimethylcyclopentane (DMCP) isomers before ring opening occurs. In this study, all of the DMCPs were lumped together as RC isomers, but it is very important to be able to distinguish the difference between these isomers, as different DMCP isomers have considerably different ONs. This effect is shown in Fig. 13. The RC step has been previously considered by many researchers, on both zeolitic and non-zeolitic supported catalysts.[60] Belatel *et al.*[61] studied reaction of MCH on Pt–Ir/sulfated zirconia and on sulfated zirconia alone. They found that the RC isomerization did

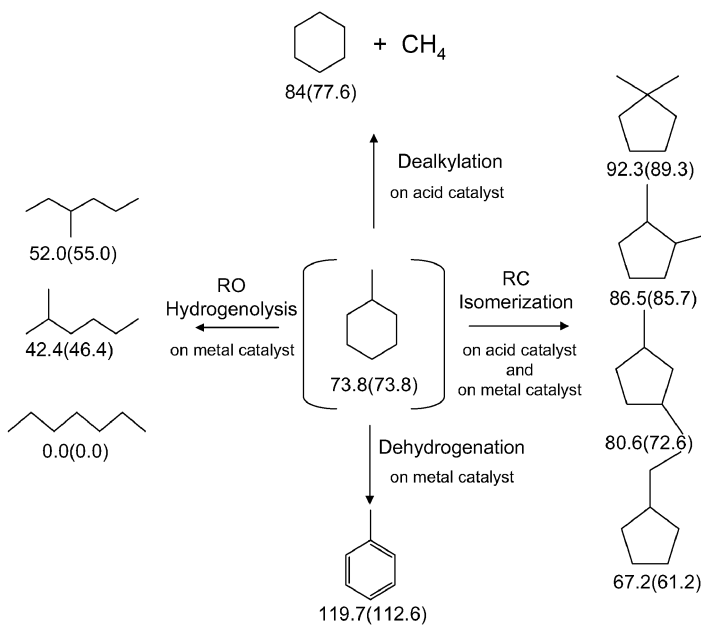

Fig. 13 Possible products from methylcyclohexane and their research octane number (RON) and their motor octane number (MON). Adapted from ref. 100.

not occur unless the metal was present on the catalyst, indicating a bifunctional pathway, which involves dehydrogenation/hydrogenation on metals.

The zeolite structure also plays a large role in RC product distribution. Weitkamp *et al.*[62] conducted experiments with Pt/HZSM-5 catalysts, which have very narrow pore sizes when compared with other zeolites, such as USY or SAPO. They found that *cis*/*trans*-1,3-dimethylcyclopentane was formed, while 1,1 and 1,2-DMCP were not. This indicates that the more oval shaped 1,3-DMCP was able to diffuse through the pores, while the more bulky and spherical isomers were not, and thus not seen in the product distribution. In short, when compared with dealkylation to cyclohexane, ring contraction of MCH is a more effective pathway to yield higher ON products. However, in order to further improve the ON, ring-opening of the RC isomers may be necessary, as shown below.

3.2.2 Metal-catalyzed ring opening. Before analyzing the RO of MCH isomers, it is worth noting that, the direct RO of MCH is not desirable, as it forms products with significant decreases in ON. This is shown in Fig. 14. The three main RO products are: *n*-heptane (RON = 0), 2-methylhexane (RON = 42), and 3-methylhexane (RON = 52). Some of the DMCP ring opening products, however have relatively high ONs, and could provide a beneficial route towards increasing the ON while eliminating aromatics in gasoline. Ring opening on metal catalysts occurs *via* hydrogenolysis, which has been previously mentioned for CN optimization. The product distribution from metal-catalyzed hydrogenolysis RO reactions is largely dependant on the nature and structure of the metal and the support, so by changing the metal particle size or the metal support interactions, the product distribution may be largely varied. As previously mentioned, while Pt particle size plays a significant role in product distribution, this effect is less pronounced for Ir catalysts. Mc Vicker *et al.*[11] have proposed that RO of alkylcyclohexanes on Ir occurs primarily *via* the dicarbene mechanism where the unsubstituted bonds are preferentially broken, and the product selectivity does not depend on dispersion. Similarly, Weisang and Gault[63] have shown that hydrogenolysis of MCP over iridium catalysts yields only branched products which result from breaking at the unsubstituted positions. Our group has found that indeed the metal particle size has little impact on the product selectivity, but the support has a significant impact.[49] The proposed dicarbene reaction path was observed to be dominant for reactions with Ir on silica,

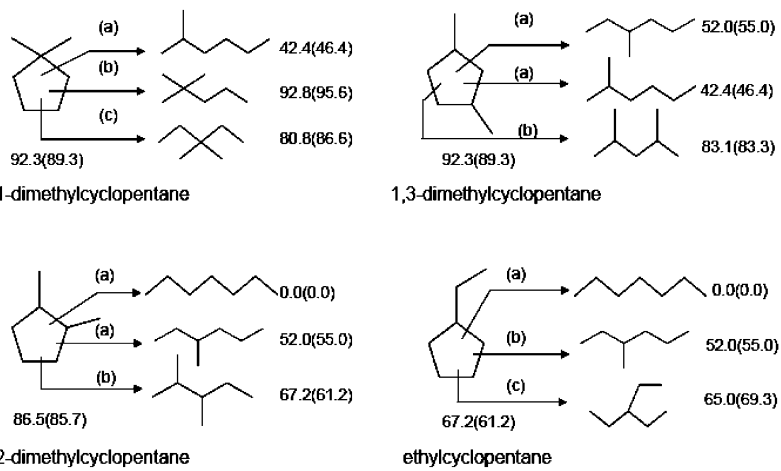

Fig. 14 Hydrogenolysis on metal catalysts: product from ring opening reactions of C7 ring contraction compounds and their corresponding research octane number and motor octane number. Adapted from ref. 100.

but when Ir/Al_2O_3 was used, the cleavage at substituted C–C bonds becomes significant.

The highly branched 1,1-dimethylcyclopentane (1,1-DMCP) not only has the highest ON among the four RC isomers, but also some of its RO products have exceptional ON (*e.g.* the RON of 1,1-dimethylpentane is 92). This product can be obtained by using metal catalysts which selectively open at secondary–secondary C–C bonds. As discussed earlier, Ir/SiO_2 is best suited for this reaction.

In summary, in order to reduce the content of toluene in gasoline while keeping a high octane number, toluene must undergo hydrogenation and ring contraction followed by SRO. The RC step can proceed *via* bifunctional catalysts and the SRO must use a metal catalyst (*e.g.* Ir/SiO_2) that is selective towards the dicarbene mechanism to cleave C–C bonds at unsubstituted positions.

4. Implementation of the catalytic strategies

As shown in the preceding section, a potential strategy to improve cetane number in streams containing aromatics would be to start with hydrogenation of the aromatic rings, and to follow with ring contraction and selective ring opening of the saturated naphthenes. In the ring opening of the naphthenic compounds, a metal catalyst should be used to selectively catalyze the cleavage of substituted C–C bond. A similar strategy could also be applied in the gasoline production if the refiner needs to remove aromatics, but without losing octane number. However, since in this case, isoparaffins with a high degree of branching are desirable, metal catalysts, which preferentially break unsubstituted C–C bonds, are the best candidates for the ring-opening step. In this section, we will review some experimental results of the individual reactions involved in these strategies. These reactions include hydrogenation, ring contraction and ring opening.

4.1 Hydrogenation

An overall solution for improving CN, ON, and TSI while meeting current environmental standards could be deep hydrogenation of aromatics. Noble metal and sulfide bimetallic catalysts are known to be very active in hydrogenation. The former exhibits the important advantage of being active at significantly lower temperatures, minimizing the severe thermodynamic limitations found at higher temperatures for any exothermic hydrogenation reaction. Therefore, in an attempt to decrease the sulfur content of fuels to the target of 15 ppm, some companies are contemplating a two-stage processing strategy in which the first stage employs a base-metal catalyst for hydrodesulfurization, while the second stage uses a low-temperature, high-activity, noble metal catalyst.[64] The hydrodesulfurization step must be done first due to the low sulfur tolerance of noble metal catalysts, although recent studies have found that bimetallic Pt–Pd catalysts supported on acidic supports can be highly tolerant to sulfur and exhibit stable hydrogenation activity under sulfur containing feeds.[68–73]

A number of publications have demonstrated the high activity of bimetallic Pt–Pd catalysts for the hydrogenation of tetralin, naphthalene and phenanthrene, which are common aromatics in the diesel range.[65–67] It has been shown that site competition is one of the most pronounced phenomena that control the hydrogenation rates. For example, the conversion of tetralin to decalin can only occur when most of the higher aromatics (phenanthrene or naphthalene) have been removed.[68] Similarly, the conversion of *cis*- to *trans*-decalin is also affected by site competition with tetralin.[65] At the same time, the sequential hydrogenation of the hydrophenanthrenes also shows the effects of site competition, with preferential reaction of the higher aromatic compounds. In the same fashion, Miura *et al.*[69] also reported the rate of hydrogenation from tetralin to decalin decreased as the content of naphthalene in the feed increased. They explained this behavior in terms of higher heat of

adsorption or stronger interaction of higher aromatic compounds with the metal surface, in agreement with recent kinetics studies.[68]

The disadvantage of noble metal catalysts for aromatics hydrogenation is their low resistance to sulfur. However, the sulfur tolerance is greatly improved when the noble metals are supported on acidic materials, such as zeolites[70,71] or acidic aluminas.[65,72] Yasuda *et al.*[73] has observed that the highest sulfur-tolerance was achieved when Pd–Pt was supported on the highest acidity USY zeolite. Other authors have also seen varying degrees of sulfur toxicity when the support acidity was modified.[74] Similarly, addition of fluorine also increases sulfur tolerance of noble metal catalysts.[65,75] Since F is very electronegative, it increases the acidity of both protonic and non-protonic sites on the catalyst surfaces.[76] Previously, our group has found that F-promoted Pt–Pd catalysts showed a higher hydrogenation activity than unpromoted catalysts. The catalyst characterization data showed that the addition of F to the alumina support helped keep the Pt–Pd alloy and prevent the formation of Pt–S bonds. The inhibition effect of the promoted catalysts was conversion-driven. At low conversions, the inhibition by sulfur was reversible, but at high conversions, the poisoning was irreversible. It has been proposed that metal–S bonds are weakened on these supports due to the electron withdrawing effect of acid sites.[77–80] In addition to the effect of the support, some researchers have investigated the addition of a second additive (*e.g.* Ge) to Pt. This promotion has also been ascribed to changes in electronic properties.[81] A different concept that does not consider the modification of the metal properties, but rather the direct participation of the acid sites has also been elaborated in some studies.[82–86] These studies show some evidence that the aromatic molecules can adsorb on acid sites where they may be hydrogenated by hydrogen that is transported from the noble metal surface by spillover. Lercher *et al.*[87–89] in a series of studies of the hydrogenation of benzene have elaborated on the role of acid site density in promoting sulfur tolerance and made a convincing argument that the adsorption of the aromatic occurs on the acid site, which is not affected by sulfur. They have expanded the concept of the direct role of the acid sites and proposed that an optimum acid site density can be found which hits a balance between an aromatic coverage high enough to cause high hydrogenation activity but not so high as to promote excessive coke formation.

4.2 Ring contraction

Hydrogenation of aromatics to saturated naphthenes is an important step in diesel fuel processing, because the CN of saturated naphthenes are much higher than those of aromatics. However, most of the CN of naphthenic compounds are lower than the minimum CN requirement of 50. Moreover, in the case of gasoline, aromatic saturation results in an important loss in ON due to the much higher ONs of aromatics than those of the corresponding naphthenes. To overcome this obstacle, researchers have suggested the ring contraction of saturated naphthenes followed by selective ring opening.[11,44]

4.2.1 Ring contraction of two-ring naphthenes. Typical molecules present in diesel fuel are alkylcyclobenzenes, alkylcyclohexanes/pentanes, and paraffins. As pointed out in our previous work,[46] neither ring contraction of the naphthenics (RC) or even one-ring opening (RO) results in increases in CN unless further selective ring opening of the second ring is involved which produces less branched paraffins such as *n*-paraffins and some iso-paraffins. The opening of alkylcyclohexanes is facilitated by an acid function in order to catalyze the isomerization of the C6 rings into the C5 ring (RC step).[90,91] Kustov *et al.*[92] also found that the acid function of the catalyst (NiW/HY) was essential for multi-ring compounds, such as decalin, but not for the one-ring cyclohexane, which can be opened on monofunctional metal catalysts (NiW/Al_2O_3).

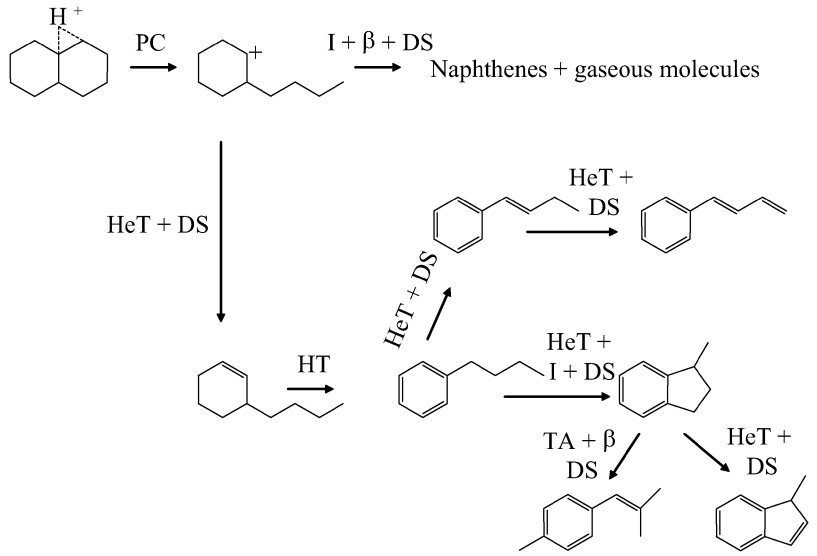

Fig. 15 A proposed reaction network of direct ring opening of decalin reaction over acidic zeolites. PC: Protolytic cracking; HeT: Hydride transfer; HT: Hydrogen transfer; I: Isomerization; β: *β*-scission; DS: Desorption; TA: Transalkylation. Adapted from ref. 47.

Among the ring opening studies of the two-fused naphthenic compounds, decalin and tetralin were widely investigated. However, only a few researchers have attempted to gain insight on the complex mechanisms responsible for the different reactions. Corma *et al.*[47] have studied the hydroconversion of decalin and tetralin over the proton-form of zeolites with different pore sizes. These authors have focused on the role of the pore size and zeolite topology in determining the product distribution. When discussing possible mechanisms of decalin conversion, they proposed that one of the paths for decalin activation might be the direct opening of the six-member ring *via* cleavage of the corresponding carbonium ion, which is initiated by the attack of a Brönsted acid site on a C–C bond described as a protolytic cracking (PC). Subsequent steps follow the typical carbenium ion reactions such as *β*-scission cracking, isomerization, and alkylation. As displayed in Fig. 15, in this proposed path, the ring opening (RO) products are the primary while the products of ring-contraction (RC) isomerization would be secondary. In a more recent investigation, Kubicka *et al.*[44,45] did not observe direct ring-opening of decalin even at low conversions and proposed that RO only occurs as a secondary reaction, which is preceded by a step of a skeletal isomerization, ring-contraction (RC). They argued against the PC of decalin as an initiation step since the RO products seem to originate only from the RC products, such as alkyl bicyclononanes (indanes) and bicyclooctanes, which acted as intermediates (see Fig. 16a and b). These secondary reactions are more evident at higher reaction temperatures. Different reaction conditions might be the cause of the opposing observations; in the former study, the decalin reaction was conducted at atmospheric pressure (0.1 MPa), high temperatures (723 K), and without added hydrogen in the feed; in the latter, the runs were conducted at higher pressures (2 MPa), lower temperatures (473–573 K), and in the presence of added H_2.

Kubica *et al.*[45] also investigated the effect of platinum-modified zeolites on the decalin reaction. They found that the addition of Pt enhances the catalyst activity. The initial isomerization was increased 3 times, which can be interpreted in terms of a change in the reaction initiation. In addition to initiation by a PC step over Brønsted acid sites, as proposed for H-form zeolites, a bifunctional initiation path

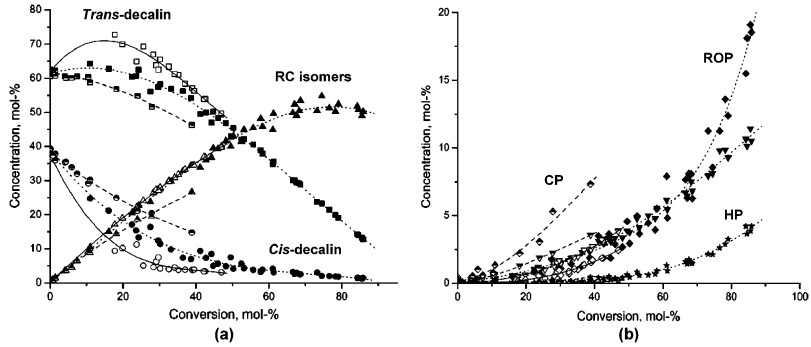

Fig. 16 Concentration of decalin and product groups as a function of conversion over H-Beta (filled), HY (open), and H-Mordenite (half-filled). CP = cracking products; ROP = ring opening products; HP = heavy products. Adapted from refs. 44 and 45.

can occur. This path includes a metal-catalyzed dehydrogenation of decalin to an olefin, which is in turn protonated on a Brønsted acid site. The formed protonated species can undergo RC and consequently RO.

The Pt-modified zeolites have much lower cracking activity and higher stability than their corresponding H-forms.[46] This change is mainly due to two factors; first, the density of Brønsted acid sites is generally lowered by the presence of Pt; second, the hydrogen transfer is greatly enhanced by Pt. The enhanced hydrogen transfer on the zeolite surface reduces the lifetime of the surface carbocations, leading to less coke and less cracking. At the same time, for the same two reasons, the presence of Pt affects the ratio of isomerization to ring opening. A comparison of Pt-modified and HY zeolites shows that the presence of Pt enhances the RC step and inhibits the RO and cracking step. This can be clearly seen in Fig. 17, which illustrates the ratio of RC/RO over HY and Pt/HY catalysts. For a given conversion, the ratio of RC/RO is higher on Pt/HY than on HY. The lower acid density and the enhanced hydrogen transfer in Pt/HY diminish the lifetime of a RC carbocation, allowing the desorption of RC products before it further converts to RO and cracking products. However, the enhancement in RC/RO ratio is only observed when Pt is located inside the zeolite channels. When it is outside the channels or in physical mixtures of HY and Pt/SiO_2 catalysts, the RC/RO ratio is the same as without Pt.

Unlike the ring opening of decalin, the RO of naphthenic compounds containing at least one benzene ring (*i.e.* tetralin, naphthalene, *etc.*) are much slower due to the presence of aromatic rings. Corma *et al.*[47] has reported differences in activity

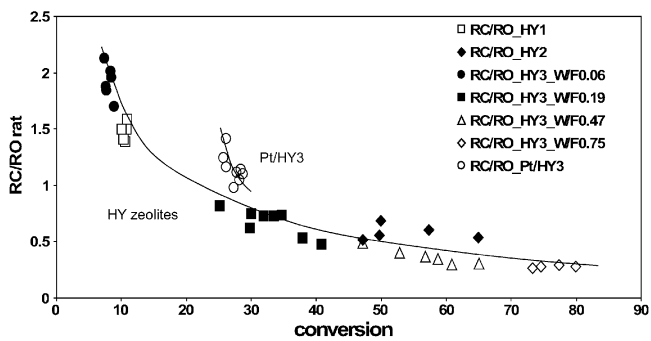

Fig. 17 RC/RO ratio of decalin ring-opening on HY zeolites and Pt/HY3 at different conversions. Conversions were varied by changing space time and time on stream. Reaction conditions: 2 MPa, 533 K, H_2 to feed molar ratio = 65. Adapted from ref. 46.

Table 3 Conversion of tetralin on physical mixtures of Pt/SiO_2 and HY catalysts. Reaction conditions: 2 MPa, 598 K, after 420 min. Adapted from ref. 46

	HY	Pt ≫ HY	HY ≫ Pt	Pt + HY, 1:1	Pt + HY, 1:2	Pt/HY
mmoles of H^+	0.26	0.16	0.16	0.16	0.25	0.09
mmoles of Pt	0.00	0.62	0.62	0.62	0.48	1.03
Tetralin conversion (%)	11.84	97.52	91.33	86.42	98.66	91.38
Products (yield, wt%)						
C1–C5	ND	ND	ND	ND	ND	ND
C6–C9	0.23	0.56	0.46	0.24	0.54	0.16
C10 products:						
Ring opening products:	3.10	8.79	3.20	5.11	12.59	12.40
Alkylcyclo compounds	0.90	8.70	2.69	4.85	12.42	11.07
Alkylbenzene	2.20	0.09	0.51	0.25	0.17	1.32
Ring contraction products:	2.26	4.13	2.50	3.34	7.08	12.73
trans-Decalin	1.05	75.31	70.46	62.04	70.63	55.43
cis-Decalin	0.61	7.06	14.01	14.48	7.76	9.69
Naphthalene	4.59	1.68	0.70	1.21	0.05	0.98

between tetralin and decalin on acidic zeolites, although these differences were not so pronounced due to high reaction temperatures (723 K) used in that study.

Our group has investigated the RO of tetralin over bifunctional Pt/HY catalysts. It was noted that tetralin first undergoes hydrogenation to decalin before the RC and RO steps. Therefore, the presence of Pt has a dramatic influence as the tetralin hydrogenation is greatly enhanced. The role of the individual functions (*i.e.* metal and acid) on the ring opening of tetralin was investigated by using physical mixtures of HY and Pt/SiO_2. The results of this study are tabulated in Table 3. In the presence of hydrogen, Pt/HY catalysts as well as the physical mixtures of HY and Pt are much more effective than HY catalysts. This result is in agreement with Arribas *et al.*,[93,94] who studied the coupled hydrogenation and RO of tetralin and 1-methylnaphthalene on Pt/USY. They concluded that the presence of Pt in the bifunctional Pt/USY catalyst significantly increased the RC rate as compared to the monofunctional USY. The same effect on the RC rate was observed by decreasing the distance between the metal and acid sites and increasing the Pt loading. In fact, if a bifunctional mechanism of RC is involved, then the proximity of Pt and acid sites can be responsible for the observed higher isomerization activity.

4.2.2 Ring contraction of one-ring naphthenes. The concept of isomerization of naphthenes (*i.e.* ring contraction) has been applied not only to the reactions relevant to diesel conversion but also to those relevant to gasoline conversion. In this section, we will discuss the ring contraction reactions concerning one-ring naphthenic compounds, which are molecules typically present in the naphtha range, used as feedstock for gasoline. Recently, McVicker *et al.*[95] investigated the isomerization reaction of MCH over Pt supported on solid acid supports, which were halided-Al_2O_3, amorphous SiO_2–Al_2O_3, and zeolites (Beta, MOR, ZSM-5, SAPO-11, ZSM-22, EU-1, ZSM-23, CLINO, and FAU). Ring contraction of MCH on acid catalysts yields four major isomers, as shown in Fig. 18. For a group of ultrastable faujasites (USYs), the acid density increases with decreasing zeolite Si/Al ratios. Consequently, the rate of MCH conversion over Pt/USY (Si/Al = 5.1) is several orders of magnitude higher than over Pt/Al_2O_3, the least active among all tested catalysts. The acid strength of the different acid catalysts investigated had a pronounced impact on the ring contraction product distributions. The equilibrium concentration of ethylcyclopentane (ECP), one of the thermodynamically least stable isomers, remains between 8 and 11% over the temperature range (473–613 K). However, at

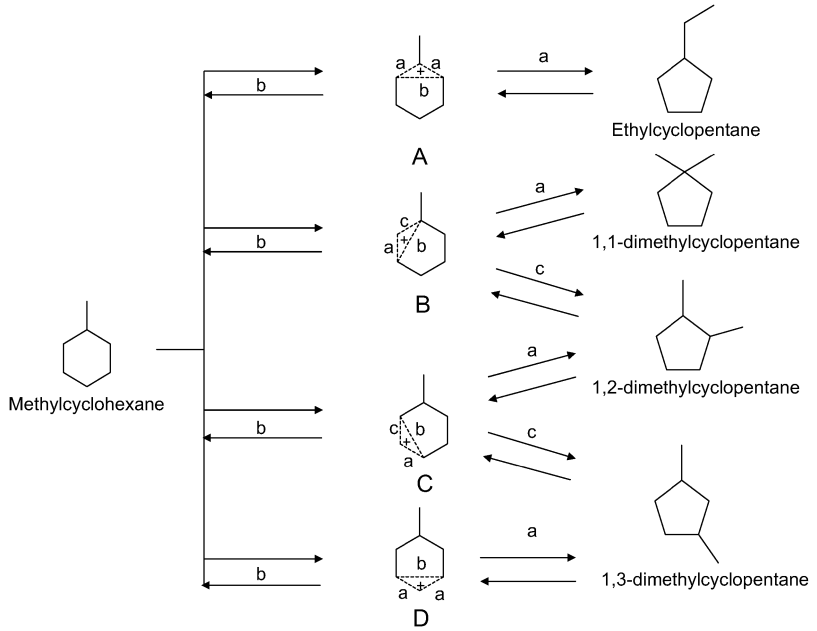

Fig. 18 Schematic diagram of ring contraction intermediates from methylcyclohexane. Adapted from ref. 95.

low conversions the product selectivity is a strong function of the catalyst acidity. For example, at the same conversion (10%) the selectivity to ECP is 55% on a Pt/SAPO catalyst of low acid strength, but only 30% on a Pt/USY (Si/Al = 5.1) catalyst of higher acidity. This pronounced difference can be ascribed to the ease of formation of the carbocation responsible for each product. The carbocation that leads to ECP is the easiest to form, as a result, when the acidity is weak, only the easiest can form.

Additionally, the *trans*-1,2-DMCP/*trans*-1,3-DMCP product selectivity ratio reflects the pore size variations of a wide range of zeolitic and microporous solid acids. Since the *trans*-1,3-DMCP isomer is smaller in size, it diffuses more easily through the 5.7 Å channel opening of ZSM-22. On the other hand, the larger *trans*-1,2-DMCP isomer will experience more difficulties in diffusing out of the channel of ZSM-22. Therefore, sterically hindered 10-ring zeolites and 10-ring microcrystalline materials such as SAPO-11 all exhibit *trans*-1,2-DMCP/*trans*-1,3-DMCP ratios of 0.5 or less. By contrast, larger pore size 12-ring zeolites and amorphous solid acids show the ratio ranging from 1.2 to 2.3.

Using MCH as probe molecule, we have put more emphasis on the role of metal in the distribution of RC isomers. The MCH reaction was studied on HY and Pt/HY catalysts. It was found that significant differences in initial activity, rate of deactivation, and product distribution were observed between the two catalysts.

Not only the stability against deactivation was higher on Pt/HY but also, the product distribution obtained on this catalyst was significantly different from that on the HY catalyst. The most obvious difference was the drastic decrease in cracking products. The RC product distribution was also much more selective to form 1-1-DMCP and ECP in the presence of Pt. This increased ECP selectivity, especially at low conversions, can be explained by the lower acid density[95] and the increased hydrogen transfer[96] that are brought about by the addition of Pt to the zeolite. The increased hydride transfer brought about by the addition of Pt has been well documented.[97–99] As shown in Fig. 18, ECP is formed from intermediate A, which is the carbocation with the lowest acid site requirement to form, and therefore, the

easiest to form. As the hydride transfer is enhanced by the presence of Pt, the surface lifetime of the carbocation is greatly reduced; thus, it does not have time to isomerize into the less favorable intermediates that would lead to 1,2 or 1,3-DMCP.

4.3 Ring opening

As suggested by some researchers,[11,100] selective ring opening following the ring contraction of naphthenic compounds can be tailored for improvement of either CN or ON. The majority of the recent work in the literature on ring opening of naphthenic compounds focuses on the improvement of CN. However, similar concepts could be applied for the improvement of ON. The only difference is that when the RO products are highly linear paraffins CN will increase and when RO products are highly branched iso-paraffins ON will increase.

As mentioned earlier, ring opening of naphthenic compounds can occur on either metal or acid catalysts. β-Scission is the typical mechanism of acid-catalyzed RO. However, acid catalysts produce excessive cracking as a side reaction, which results in loss of molecular weight and CN. Therefore, in this section, only metal-catalyzed RO (hydrogenolysis) is discussed. RO on metal catalysts can operate *via* three main mechanisms: dicarbene, π-adsorbed olefin, and metallocyclobutane, which are illustrated in Fig. 19 (using dimethylcyclohexane as a model naphthenic molecule). Gault *et al.*[55] first introduced the concept of metallocyclobutane intermediates in the ring opening of methylcyclopentane. He concluded that the reaction path involving the metallocyclobutane intermediate had an activation energy higher than that involving dicarbene intermediates. Later, in good agreement with this hypothesis, Foger *et al.*[101,102] found that the activation energy for the dicarbene mode is significantly lower than that for the π-adsorbed olefin mode. These authors observed an activation energy of 170 kJ mol^{-1} for the *n*-butane hydrogenolysis, a typical dicarbene reaction, and a much higher activation energy (240 kJ mol^{-1}) for the hydrogenolysis of neopentane, which cannot undergo hydrogenolysis *via* the dicarbene mechanism.

Depending on the noble metal, particle size, and the dispersion of the metal catalyst used, specific mechanisms may become dominant in a given case. For instance, on Pt catalysts,[103–106] the dicarbene mode is favored when large ensembles of active sites are available; by contrast, when the ensembles are broken up by surface dilution, the dicarbene mode is suppressed, and consequently the π-adsorbed olefin or metallocyclobutane mode takes over. Similarly, the use of bimetallic catalysts demonstrated a similar shift to more substituted C–C cleavage as the density of the large ensemble of sites was diluted with unreactive metals such as Ag or Cu.[107,108] Within a series of noble metals investigated by Gault *et al.*, iridium exhibited the strongest preference for the dicarbene mode. Moreover, it was observed that this tendency did not change with particle size. Likewise, Ponec *et al.*[109] found no significant effect of particle size in ring opening reactions over Ir catalysts of various dispersions, but reported that Ir became more selective towards ring opening at substituted (tertiary) carbon centers as the catalyst became covered by carbonaceous species. Similarly, as mentioned above, we have found that the

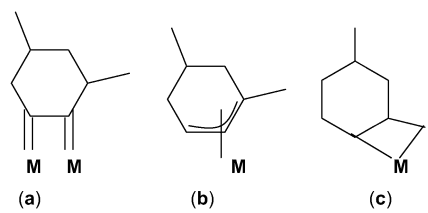

Fig. 19 Ring opening modes: dicarbene (a), π-adsorbed olefin (b), metallocyclobutane (c). Adapted from ref. 49.

product distribution for DMCH ring opening did not depend so much on Ir particle size, but was greatly affected by the type of support used.[49]

4.3.1 Ring opening of two-ring naphthenes. As shown in Fig. 1, if the opening of two-ring naphthenic compounds is selective to produce one-ring naphthenes and subsequently highly linear alkanes, the gain in CN can be substantial. Ring opening of decalin, which is a typical two-ring compound with carbon number in the diesel range, has been extensively studied. However, most of these studies were carried out on acid or bifunctional catalysts, where isomerization of decalin was followed by ring opening. Direct RO of decalin on metal catalysts has been reported by McVicker *et al.*[11] As already mentioned, they found that RO of 6-membered rings is much slower than that of 5-membered rings. Under the same reaction conditions, while conversion of decalin was only 4.4%, that of perhydroindane, which contains one 6- and one 5-membered ring, was 68%. In both cases, the RO of products were only alkylcyclohexanes; that is perhydroindane opened at the C5 ring only. On the other hand, bicyclo[3,3,0]octane, which contains two saturated 5-membered rings, yielded both one-ring naphthenes and acyclic paraffins as RO products, indicating that either one or two C5 rings opened. This difference is due to a higher stability of the six-member rings compared to the five-member ring. Estimated ring strain energies are about 1 kcal mol^{-1} and 6–7 kcal mol^{-1}, for the C6 and C5 rings, respectively.[110]

In another study involving RO on iridium catalysts, Nylen *et al.*[111] have reported the ring opening of indan on monometallic and bimetallic Ir–Pt prepared by the microemulsion method. The main reaction product observed over these catalysts was 2-ethyltoluene, which results from cleavage at unsubstituted C–C bonds. By contrast, *n*-propylbenzene, a product resulting from cleavage at the substituted C–C bonds, was only formed in smaller quantities. According to Gault *et al.*,[55] in most hydrogenolysis reactions, iridium catalysts only exhibit dicarbene characteristics regardless of the particle sizes. Meanwhile, on Pt catalysts, both dicarbene and substituted C–C breaking modes can be operative, depending on the particle size. In this case, ethylbenzene was dominant for all three catalysts. Similarly, the selectivity of *n*-propylbenzene was slightly higher for the monometallic Pt catalyst than for the two containing iridium.

These observations can be explained taking into consideration that in this study the metal particle sizes were relatively large in all three catalysts, so the dicarbene mechanism dominated, even on the Pt-based catalysts. In any case, a somewhat higher selectivity towards substituted C–C cleavage was observed on the Pt catalysts, relative to the monometallic Ir catalyst. However, as we have recently pointed out, unless the naphthenic rings are opened very selectively at the substituted C–C bonds, no considerable gain in CN can be achieved by RO. This was not the case in any of the Pt–Ir catalysts presented in ref. 111.

4.3.2 Ring opening of one-ring naphthenes. The CN of straight-chain alkylcyclohexanes, which can be produced by RO of two-ring naphthenes, are higher than the original feeds. However, in order to obtain higher CN products, opening the second ring to highly linear alkanes is imperative. Many researchers have studied the RO of one-ring naphthenes on noble metal catalysts. In order to understand how the presence of alkanes in the processing feedstocks containing different compounds such as alkanes, naphthenes, *etc.*, modifies the RO of polycyclonaphthenes to alkylnaphthenes, or alkanes, Coq *et al.*[51] has investigated the competition reaction of methylcyclohexane (MCH) and *n*-hexane (*n*-C6) over alumina-supported Pt, Ir, Ru catalysts. They concluded that the conversion of *n*-C6 is strongly inhibited in the presence of MCH, which remains the most abundant reactant adsorbed on the metal particles. In contrast, neither the activity nor the selectivity for MCH conversion was affected by the presence of *n*-C6 in the feed. The only observed reaction of MCH on

Pt catalysts was the dehydrogenation to toluene, which was independent of catalyst particle size. Meanwhile, the selectivity for RO of MCH on iridium and ruthenium was 50% and RO was found to occur only at unsubstituted C–C bonds.

In parallel, McVicker *et al.*[11] have observed similar product distributions while studying the RO of MCH on four different catalysts—0.6% Pt/SiO_2, 15% Ni/Al_2O_3, 1.5% Ru/SiO_2, and 0.9% Ir/Al_2O_3. Since the reaction was operated at high pressure, RO was the major reaction instead of dehydrogenation to toluene, as in the previous example. *n*-Heptane, a product of C–C bond cleavage at the substituted position was the most abundant product on the Pt catalyst, showing the preference on this metal for opening at secondary–tertiary C–C bonds. By contrast, dicarbene products, *i.e.* methylhexanes, were the main products of the RO of MCH on the Ni, Ru and Ir catalysts. Although on Ir catalysts the dicarbene mode dominates in the MCH conversion its contribution is not as pronounced in the conversion of a highly substituted molecule such as 1,2,4-trimethylcyclohexane (1,2,4-TMCH). In this case, six nonane isomers (one from each C–C bond in the ring) can be generated from RO. Among them 2,3,5-trimethylhexane, which results from the cleavage of the single unsubstituted secondary–secondary C–C bond in the molecule accounts for about 35%, which is still greater than the statistical percentage (17%). Among the RO products originating from breaking the substituted C–C bonds, those from the half of the molecule containing the two contiguous methyl groups were much more abundant than those originating from cleavage on the other half. As suggested by the authors, a change in mechanism may occur for highly substituted cyclohexyl rings. It is possible that methyl substituents activate the ring in a way that favors the rupture of substituted C–C bonds.

To gain further understanding on how the dispersion of the iridium catalyst influences the ring opening of highly substituted cyclohexanes, we have studied the ring opening of 1,3-dimethylcyclohexane (1,3-DMCH) on different supported iridium catalysts. The ring opening of 1,3-DMCH over iridium generates three primary products: 2-methylheptane (2-MC7), 4-methylheptane (4-MC7), and 2,4-dimethylhexane (2,4-DMC6), which result from the C–C opening of the ring at different positions (see inset in Fig. 20). While 2-MC7 and 4-MC7 arise from the breakage of tertiary-secondary C–C bonds (bonds *a* and *b* in Fig. 20), 2,4-DMC6 is formed by cleavage of a secondary–secondary C–C bond (bonds c). As described in a recent contribution, we were able to predict the CNs of products, such as those indicated by cleavage at bonds *a*, *b*, and *c* (47, 40, and 31, respectively). Starting with a CN of the original feed of 30, cleavage at both the *a* and *b* positions, but not at *c*, results in desirable products.

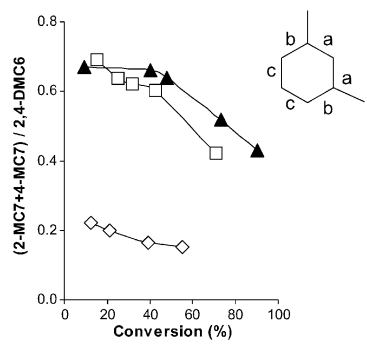

Fig. 20 Ratio of substituted C–C cleavage to unsubstituted C–C cleavage of 1,3-DMCH over Ir on different supports. Reaction was conducted at 593 K and 3540 kPa. Hydrogen to hydrocarbon ratio was kept at 30. Without considering secondary hydrogenolysis, the ratio (2-MC7 + 4-MC7)/ 2,4-DMC6 would represent the ratio of $(a + b)/c$ cleavage. The statistical value of $(a + b)/c$ is 2. ▲ = Ir/Al_2O_3; ◇ = Ir/SiO_2; □ = Ir/TiO_2. Adapted from ref. 49.

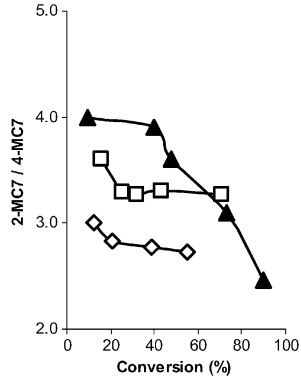

Fig. 21 Ratio of substituted C–C cleavage at internal to external positions of 1,3-DMCH over Ir on different supports. Reaction was conducted at 593 K and 3540 kPa. Hydrogen to hydrocarbon ratio was kept at 30. Without considering secondary hydrogenolysis, the ratio 2-MC7/4-MC7 would represent the ratio of a/b cleavage. ▲ = Ir/Al_2O_3; ◇ = Ir/SiO_2; □ = Ir/TiO_2. Adapted from ref. 49.

In search for a catalyst that yields high-cetane products, we compared Ir catalysts on three different supports. The results are summarized in Fig. 20. Without considering secondary hydrogenolysis, the ratio (2-MC7 + 4-MC7)/2,4-DMC6 would represent the ratio of $(a+b)/c$ cleavage. Accordingly, the statistical value of $(a + b)/c$ is 2. The observed trend is as follows: $Ir/Al_2O_3 \approx Ir/TiO_2 \gg Ir/SiO_2$. Thus, for CN improvement, titania or alumina supports should be used. Conversely, if the desired property is the octane number, then the most effective support would be silica. Although the ratio of $(a + b)/c$ cleavage is not as high as the statistical value of 2, there are considerable amounts of 2-MC7 and 4-MC7, which are originated from breaking of tertiary-secondary C–C bonds, produced. This is in a good agreement with what was observed in the reactions of 1,2,4-TMCH by McVicker *et al.*[11] and highly-substituted cyclopentanes by Gault *et al.*[55] The addition of methyl groups decreased the difference in activation energy between the metallocyclobutane and dicarbene modes. It is clearly shown here that this trend works not only for substituted cyclopentanes (C5 rings), but also for cyclohexanes (C6 rings). This behavior points toward the metallocyclobutane mechanism since such intermediate is one in which external methyl groups may be directly involved in the ring opening.

Furthermore, it is observed that the chance of breaking the substituted C–C bond inside (position *a*) and outside (position *b*) the two methyl groups also varies when the support is changed. The ratio a/b is also important, because there is a significant difference in the CN of the product obtained by each of the two substituted C–C bonds. In terms of cetane numbers, a high a/b ratio is desirable. As shown in Fig. 20, the Ir/Al_2O_3 catalyst shows the highest (2-MC7/4-MC7) ratio, but this ratio decreases significantly with increasing conversion due to the secondary hydrogenolysis of the primary products. Meanwhile, this ratio stays relatively constant for the other two catalysts. If there were no preferential cleavage for the two possible substituted C–C bonds, then the statistical ratio for a/b would be equal to unity (2/2). However, as shown in Fig. 21, the ratio is >2 at all conversions and can be as high as 4 for some catalysts at low conversions. It is then concluded that the C–C bond inside the two methyl substituents (a) is preferentially ruptured in comparison with the C–C bonds outside the groups (b). It should be appreciated that the addition of methyl substituents not only enhances the rate of ring opening of C6 rings, but also contributes positively to the ring opening at the more sterically hindered C–C bond (external to methyl groups).

In the same contribution, we investigated the effects of varying the reduction temperature. Fig. 22 shows the evolution of the (2-MC7 + 4-MC7)/2,4-DMC6 ratio

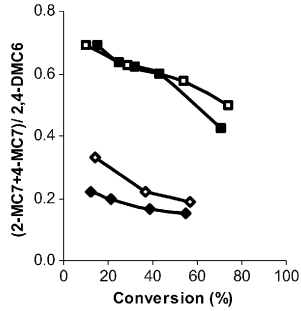

Fig. 22 RO of 1,3-DMCH: (2-MC7 + 4-MC7) / 2,4-DMC6 ratio with LTR (593 K) and HTR (723 K) catalysts. Reaction was conducted at 593 K and 3540 kPa. Hydrogen to hydrocarbon ratio was kept at 30. ◇ = Ir/SiO_2-LTR; □ = Ir/TiO_2-LTR; ◆ = Ir/SiO_2-HTR; ■ = Ir/TiO_2-HTR. Adapted from ref. 49.

as a function of 1,3-DMCH conversion over Ir/SiO_2 and Ir/TiO_2 catalysts after low- and high temperature reduction. While in the case of TiO_2-supported catalysts there was little difference between low-temperature and high-temperature reduction, a substantial loss in selectivity was observed on the SiO_2-supported catalyst after reduction at 723 K. This difference may be due to the greater decrease in metal dispersion occurring on the SiO_2-supported catalyst at high temperatures than on the other support. Similarly, the 2-MC7/4-MC7 ratios shown in Fig. 23 for these two catalysts after different reduction treatments seem to differ significantly as a function of reduction temperature. While the effect of reduction temperature is not significant at low conversions, the difference becomes more pronounced with increasing conversion, indicating that the high-temperature reduction preferentially inhibits the secondary hydrogenolysis of 2-MC7. As a result, the 2-MC7/4-MC7 ratio does not decrease as much with 1,3-DMCH conversion over the catalysts reduced at high temperature as over the catalysts reduced at lower temperatures. This tendency appears advantageous for maintaining high CN at high conversions.

4.4 Combination of ring contraction and ring opening to maximize fuel properties

As proposed in Section 3.2, ring contraction of MCH followed by ring opening of RC isomers can be an attractive strategy to obtain high ON products with low

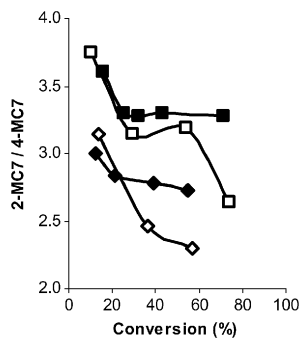

Fig. 23 Ratio of substituted C–C cleavage at internal to external positions of 1,3-DMCH over Ir catalysts reduced at different temperatures; LTR = 593 K; HTR = 723 K. Reaction was conducted at 593 K and 3540 kPa. Hydrogen to hydrocarbon ratio was kept at 30. Without considering secondary hydrogenolysis, the ratio 2-MC7/4-MC7 would represent the ratio of a/b cleavage. ◇ = Ir/SiO_2-LTR, □ = Ir/TiO_2-LTR, ◆ = Ir/SiO_2-HTR, ■ = Ir/TiO_2-HTR. Adapted from ref. 49.

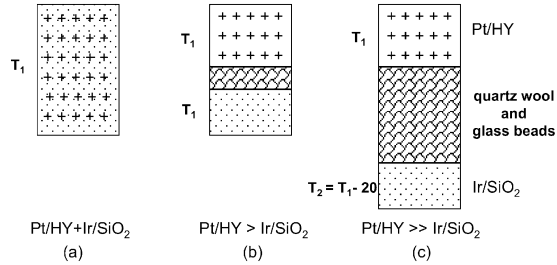

Fig. 24 Schematic reaction system configurations. Adapted from ref. 100.

aromatics content. In this case, the ring opening should be selective towards cleavage at unsubstituted secondary–secondary C–C bonds to produce highly branched iso-paraffins. In our recent work,[100] we have displayed a set of experiments with different bed configurations (see Fig. 24). Configuration (a) represents a physical mixture of Pt/HY and Ir/SiO_2 (Pt/HY + Ir/SiO_2), (b) a dual bed configuration with the Pt/HY bed followed by the Ir/SiO_2 bed (Pt/HY $\Rightarrow$ Ir/SiO_2) with the two beds at the same temperature, and (c) the same dual bed confirmation (Pt/HY $\Rightarrow$ Ir/SiO_2), but in this case the temperature of the Pt/HY bed is kept 20 °C higher than the Ir bed.

The effect of the different strategies on the resulting RON and MON can be compared in a more quantitative way by inspecting the evolution of octane number. To obtain the octane numbers of the product mixtures we used the method developed by Ghosh *et al.*[14] (described in Section 2.4). As shown in Fig. 25a and b, it can be observed that the calculated octane numbers, RON and MON, in the sequential beds (b and c) are higher than that of the physical mixture (a). For the physical mixture (a), some C6 RO occurs, which produces undesirable products, but as for the two stage bed configurations (b) and (c), some of the MCH was isomerized to RC products in the Pt/HY bed, which then formed C5 RO products as the increased ring strain makes it very easy to open the C5 rings at lower temperatures. This two bed approach therefore yields higher fractions of high octane dimethylpentanes resulting from the MC5 ring cleavage. The downside of configuration (b) where both reactors are kept at the same temperature is that in order to avoid C6 RO, lower temperatures must be used, which result in lower conversions. Furthermore, at higher temperatures (*e.g.* 573 K) besides the undesired C6 RO, large amounts of cracking products are also produced, which lead to undesirable volume losses. Consequently, a drop in RON and MON was observed as MCH conversion

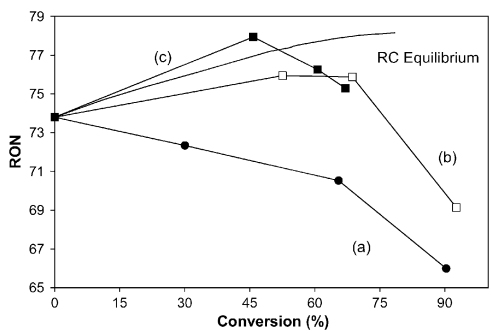

Fig. 25 RON of the product mixture as a function of MCH conversion, calculated by the method of ref. 14. Standard errors for this method are $\sim\pm$1RON. For the product distribution obtained on the three Pt/HY + Ir/SiO_2 catalyst bed configurations illustrated in Fig. 24. Conversion was varied by changing temperature. Total pressure = 2 MPa; H_2/feed molar ratio = 40. Adapted from ref. 100.

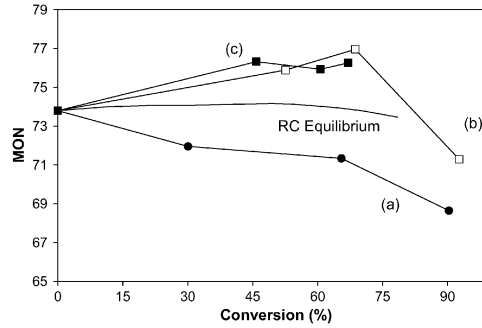

Fig. 26 MON of the product mixture as a function of MCH conversion, calculated by the method of ref. 14. Standard errors for this method are $\sim \pm 1$MON. For the product distribution obtained on the three Pt/HY + Ir/SiO_2 catalyst bed configurations illustrated in Fig. 24. Conversion was varied by changing temperature. Total pressure = 2 MPa; H_2/feed molar ratio = 40. Adapted from ref. 100.

increases. Unlike the configuration (b), in the reactor configuration with well-separated catalysts, case (c), breaking the C–C bond of MCH can be prevented by keeping the second bed at a lower temperature. In this way, the C–C bond cleavage of the C5-member rings, with lower activation energy, is preferentially accomplished. However, while the total MCH conversion increases with temperature, the direct opening of the C6-member ring starts to occur on both reactor configurations, which generates the low-octane alkane products (*n*-heptane, 2-methylhexane, 3-methylhexane, and 3-ethylpentane), which result in decrease of both RON and MON (see Fig. 26a and b).

Therefore, a potential strategy for maximizing RON and MON would be a first reactor containing a bifunctional catalyst (*e.g.* Pt/HY) that maximizes the conversion to ring contraction products, but avoids cracking, followed by a second bed with a ring opening catalyst that maximizes the C–C bond cleavage at unsubstituted positions, but does not undergo multiple hydrogenolysis (*e.g.* Ir/SiO_2).

5. Concluding remarks

The increasingly severe environmental standards on petroleum fuels place new problems to refiners around the world. The high cetane numbers required in diesels as well as the elimination of aromatics from gasolines while maintaining high octane number posse a significant challenge. As it has been the case for many years, catalytic strategies can help the refiner overcome these challenges. In this contribution we have illustrated the application of a combination of methods to maximize either cetane or octane number. The approach incorporates the prediction of the particular fuel property for pure compounds and hydrocarbon mixtures. This prediction makes possible the identification of specific reaction paths that maximize the desired property. Naphthenic molecules such as alkylcyclohexanes and alkyldecalins are compounds that mainly come from hydrogenation of the corresponding aromatics. In general, they have neither high cetane nor octane numbers. Significant increases in each of these properties can be gained if the proper C–C bond is broken. Cleavage of an unsubstituted C–C bond usually brings about an increase in octane number, since a branched isoparaffin is obtained. By contrast, C–C cleavage at a substituted position results in an increase in cetane number, since this cleavage reduces the number of branches.

To accomplish these tailored C–C bond cleavages in a controlled fashion, the researcher has the option of working with acidic, bifunctional or metallic catalysts that can carry out the proper reaction. In particular, a balanced combination of a

ring contraction catalyst followed by a ring opening catalyst with the right selectivity appears as a powerful approach.

Acknowledgements

We gratefully acknowledge the Oklahoma Center for Advancement of Science and Technology (OCAST) and ConocoPhillips for support of this work.

References

1 W. W. Lange, J. A. Cooke, P. Gadd, H. J. Zurner, H. Schlogl and K. Richter, *Society of Automotive Engineers, [Special Publication] SP*, 1997, SP-1302.
2 E. G. Barry, L. J. McCabe, D. H. Gerke, J. M. Perez, SAE-Paper, 852078, pp. 11–33.
3 In "Summary and Analysis of Comments: Control of Emissions from on Road Diesel Engines", EPA 420-R-04-008, May 2004.
4 In "Proposal for a Directive of The European Parliament and of The Council on the quality of petrol and diesel fuels and amending Directive 98/70/EC" by Commission of The European Communities, Brussels, 2001.
5 B. D. Cooper, *Appl. Catal. A-Gen.*, 1996, **137**(2), 203.
6 M. Kagami, Y. Akasaka, K. Date, T. Maeda, SAE-Paper, 841082, 1984.
7 S. L. Lee, P. H. Desai, C. C. Jonhnson and M. Y. Asim, *Fuel Reformulation*, 1993, **3**(3), 26.
8 K. Parikh, *Bull. Catal. Soc. India*, 2004, **3**, 68.
9 A. Roj and K. Karlsson, *Fuels Reformulation*, 1998, **46**.
10 M. Wilson, I. Fisher and J. Kriz, *Ind. Eng. Chem. Prod. Res. De.*, 1986, **25**(4), 505.
11 G. McVicker, M. Daage, M. Touvelle, C. Hudson, D. Klein and W. Baird, *J. Catal.*, 2002, **210**(1), 137.
12 R. C. Santana, P. T. Do, W. E. Alvarez, J. D. Taylor, E. L. Sughrue and D. E. Resasco, *Fuel*, 2006, **85**, 643.
13 A. M. Aitani, *Int. J. Hydrogen Energy*, 1996, **21**(4), 267.
14 P. Ghosh, K. J. Hickey and S. B. Jaffe, *Ind. Eng. Chem. Res.*, 2006, **45**(1), 337.
15 R. Meusinger and R. Moros, *Chem. Intell. Lab. Syst.*, 1999, **46**, 67.
16 T. D. B. Morgan, G. J. Den Otter, W. W. Lange, J. Doyon, J. R. Barnes, T. Yamashita, SAE-paper, 932678, 1993.
17 A. Petit, X. Montagne, SAE-paper, 932681, 1993.
18 In "Regulation of Fuel and Fuel Additives: Extension of California Enforcement Exemptions for Reformulated Gasoline to California Phase 3 Gasoline". EPA, Federal Register, 2005, **70**(244), 75914.
19 O. L. Gulder, *Combust. Flame*, 1989, **78**(2), 179.
20 D. B. Olson, J. C. Pickens and R. J. Gill, *Combust. Flame*, 1985, **62**(1), 43.
21 R. A. Hunt, Jr, *J. Ind. Eng. Chem.*, 1953, **45**, 602–6.
22 R. L. Schalla and G. E. McDonald, *J. Ind. Eng. Chem.*, 1953, **45**, 1497.
23 H. F. Calcote and D. M. Manos, *Combust. Flame*, 1983, **49**(1–3), 289.
24 In "Fuel Compositions for Homogeneous Charge Compression Ignition Engines". Eur. Pat. Appl., No: EP1371715, 2003.
25 A. Stanislaus and B. H. Cooper, *Catal. Rev. Sci. Eng.*, 1994, **36**, 75.
26 M. K. Nandi, D. C. Jacobs, F. J. Liotta, H. S. Kesling, SAE-paper Sp-1056, 1994, 105.
27 G. Suppes, Z. Chen, Y. Rui, M. Mason and J. Heppert, *Fuel*, 1999, **78**(1), 73.
28 R. L. McCormick, J. R. Alvarez, M. S. Graboski, Colorado Institute for Fuels and Engine Research, C. S. O. M. G., Colorado, NREL; 2003, 1 [report 6].
29 J. M. Luco and E. Marchevsky, *Curr. Comput.-Aided Drug Des.*, 2000, **2**(1), 31.
30 R. P. Verma, *Mini-Rev. Med. Chem.*, 2006, **6**(4), 467.
31 H. Yang, Z. Ring, Y. Briker, N. Mclean, W. Friesen and C. Fairbridge, *Fuel*, 2002, **81**(1), 65.
32 N. Ladommatos and J. Goacher, *Fuel*, 1995, **74**(7), 1083.
33 P. Ghosh and S. B. Jaffe, *Ind. Eng. Chem. Res.*, 2006, **45**(1), 346.
34 J. D. Taylor, J. Michael, in "Compendium of Experimental Cetane Number Data", 2004. Golden, Colorado: National Renewable Energy Laboratory, 48.
35 T. A. Albahri, *Ind. Eng. Chem. Res.*, 2003, **42**, 657.
36 D. Billingsley, L. Gordon, Z. Tzanzalian, in "Octane Prediction of Gasoline Blends Using Neural Nets", 1995, Nashville, NPRA Computer Conference.
37 P. C. Anderson, J. M. Sharkey and R. P. Walsh, *J. Inst. Pet.*, 1972, **59**, 83.
38 E. J. Y. Scott, *Proc. API DiV. Refin.*, 1958, **38**, 90.

39 S. Yan, E. G. Eddings, A. B. Palotas, R. J. Pugmire and A. F. Sarofim, *Energy Fuels*, 2005, **19**(6), 2408.
40 K. Nakakita, K. Akihama, W. Wssman and J. T. Farrell, *Ind. J. Engine Res.*, 2005, **6**(3), 187.
41 I. P. Androulakis, M. D. Weisel, C. S. Hsu, K. Qian, L. A. Green and J. T. Farrell, *Energy & Fuels*, 2005, **19**, 111.
42 Y. Akasaka and Y. Sakurai, *Trans. JSME*, 1997, **63**(607), 1091.
43 B. M. Fabuss, J. O. Smith and C. N. Satterfield, *Adv. Pet. Chem. Refin.*, 1964, **9**, 157.
44 D. Kubicka, N. Kumar, P. Maki-Arvela, M. Tiitta, V. Niemi and T. Salmi, *J. Catal.*, 2004, **222**(1), 65.
45 D. Kubicka, N. Kumar, P. Maki-Arvela, M. Tiitta, V. Niemi and H. Karhu, *J. Catal.*, 2004, **227**(2), 313.
46 M. Santikunaporn, J. E. Herrera, S. Jongpatiwut, D. E. Resasco, W. E. Alvarez and E. L. Sughrue, *J. Catal.*, 2004, **228**(1), 100.
47 A. Corma, V. Gonzalez-Alfaro and A. Orchilles, *J. Catal.*, 2001, **200**(1), 34.
48 T. Demuth, P. Raybaud, S. Lacombe and H. Toulhoat, *J. Catal.*, 2004, **222**(2), 323.
49 P. T. Do, W. E. Alvarez and D. E. Resasco, *J. Catal.*, 2006, **238**(2), 477.
50 D. Teschner, D. Duprez and Z. Paal, *J. Mol. Catal. A: Chem.*, 2002, **179**(1–2), 201.
51 C. G. Walter, B. Coq, F. Figueras and M. Boulet, *Appl. Catal. A: Gen.*, 1995, **133**(1), 95.
52 K. Foger and J. R. Anderson, *J. Catal.*, 1979, **59**(3), 325.
53 B. Coq, A. Bittar and F. Figueras, *Appl. Catal.*, 1990, **59**(1), 103.
54 P. Esteban Puges, F. Garin, F. Weisang, P. Bernhardt, P. Girard, G. Maire L. Guczi and Z. Schay, *J. Catal.*, 1988, **114**(1), 153.
55 F. G. Gault, *Adv. Catal.*, 1981, **30**, 1.
56 B. Coq, E. Crabb and F. Figueras, *J. Mol. Catal. A-Chem.*, 1995, **96**(1), 35.
57 R. M. Roberts, H. H. Chen and B. Junhasavasdikul, *J. Org. Chem.*, 1978, **43**(15), 2977.
58 A. V. Mashkina and V. I. Chernov, *Kinet. Catal.*, 2005, **46**(1), 88.
59 S. Mignard, P. H. Caillette and N. Marchal, *Chem. Ind.*, 1994, **58**, 447.
60 F. Figueras, B. Coq, C. Walter and Jean-Yves Carriat, *J. Catal.*, 1997, **169**, 103.
61 H. Belatel, H. Al-Kandari, F. Al-Khorafi, A. Katrib and F. Garin, *Appl. Catal. A*, 2004, **275**, 141.
62 J. Weitkamp, P. A. Jacobs and S. Ernst, in *"Structure and Reactivity of Modified Zeolites"*, Elsevier Sci. Publ., 1984, p. 279.
63 F. Weisang and F. G. Gault, *Chem. Comm.*, 1979, **519**.
64 C. Song and X. Ma, *Appl. Catal. B*, 2003, **41**, 207.
65 S. Jongpatiwut, Z. Li, D. E. Resasco, W. E. Alvarez, E. L. Sughrue and G. W. Dodwell, *Appl. Catal. A: Gen.*, 2004, **262**(2), 241.
66 R. M. Navarro, B. Pawelec, J. M. Trejo, R. Mariscal and J. L. G. Fierro, *J. Catal.*, 2000, **189**, 184.
67 A. D. Schmitz, G. Bowers and C. Song, *Catal. Today*, 1996, **31**, 45.
68 R. C. Santana, S. Jongpatiwut, W. E. Alvarez and D. E. Resasco, *Ind. & Eng. Chem. Research*, 2005, **44**, 7928.
69 K. Ito, Y. Kogasaka, H. Kurokawa, M. Ohshima, K. Sugiyama and H. Miura, *Fuel Process. Technol.*, 2002, **79**(1), 77.
70 H. Yasuda and Y. Yoshimura, *Catal. Lett.*, 1997, **46**(1–2), 43.
71 B. Pawelec, R. Mariscal, R. M. Navarro, S. Van Bokhorst, S. Rojas and J. L. G. Fierro, *Appl. Catal. A: Gen.*, 2002, **225**(1–2), 223.
72 W. Qian, H. Shirai, M. Ifuku, A. Ishihara and T. Kabe, *Energy & Fuels*, 2000, **14**, 1205.
73 H. Yasuda, N. Matsubayashi, T. Sato and Y. Yoshimura, *Catal. Lett.*, 1998, **54**, 23.
74 T. Fujikawa, K. Idei, K. Ohki, M. Mizuguchi and K. Usui, *Appl. Catal. A: Gen.*, 2001, **205**, 71.
75 R. J. White, R. J. Houston, U.S. Patent 3435085, 1969.
76 A. K. Ghosh and R. A. Kydd, *Catal. Rev. Sci. Eng.*, 1985, **27**, 539.
77 R. A. Dalla Betta and M. Boudart, *Proc. 5th Int. Congr. Catal.*, 1972, 1329.
78 S. T. Homeyer and W. M. H. Sachtler, *Stud. Surf. Sci. Catal.*, 1989, **40**, 975.
79 J. K. Lee and H. K. Rhee, *J. Catal.*, 1998, **208**, 177.
80 D. C. Koningsberger, J. de Graaf, B. L. Mojet, D. E. Ramaker and J. T. Miller, *Appl. Catal. A: Gen.*, 2000, **205**, 191.
81 S. M. Kovach, G. D. Wilson, US Patent Appl. 3 943 053, 1974.
82 P. Chou and M. A. Vannice, *J. Catal.*, 1987, **107**, 129.
83 S. D. Lin and M. A. Vannice, *J. Catal.*, 1993, **143**, 539.
84 M. V. Rahaman and M. A. Vannice, *J. Catal.*, 1991, **127**, 251.
85 J. Wang, Q. Li and J. Yao, *Appl. Catal. A*, 1999, **184**, 181.
86 J. Chupin, N. S. Gnep, S. Lacombe and M. Guisnet, *Appl. Catal. A*, 2001, **206**, 43.
87 L. J. Simon, J. G. Van Ommen, A. Jentys and J. A. Lercher, *J. Catal.*, 2001, **203**(2), 434.

88 L. J. Simon, J. G. Van Ommen, A. Jentys and J. A. Lercher, *Stud. Surf. Sci. Catal.*, 2001, **135**, 4400.
89 L. J. Simon, J. G. Van Ommen, A. Jentys and J. A. Lercher, *J. Catal.*, 2001, **201**, 60.
90 G. B. M. Daage, M. S. McVicker, C. W. Touvelle, D. P. Hudson, B. R. Klein, J. G. Cook, S. Chen, D. E. W. Hantzer and E. S. Vaughan, *Stud. Surf. Sci. Catal.*, 2001, **135**, 159.
91 H. Schulz, J. Weitkamp and H. Eberth, *Proc. 5th Int. Congr. Catal.*, 1973, **2**, 1229.
92 L. M. Kustov, A. Yu. Stakheev, T. V. Vasina, O. V. Masloboishchikova, E. G. Khelkovslaya-Sergeeva and P. Zeuthen, *Stud. Surf. Sci. Catal.*, 2001, **138**, 307.
93 M. A. Arribas, P. Concepcion and A. Martinez, *Appl. Catal. A: Gen.*, 2004, **267**, 111.
94 M. A. Arribas and A. Martınez, *Stud. Surf. Sci. Catal.*, 2000, **130**, 2585.
95 G. B. McVicker, O. C. Feeley, J. J. Ziemiak, D. E. W. Vaughan, K. C. Strohmaier, W. R. Kliewer and D. P. Leta, *J. Phys. Chem. B*, 2005, **109**, 2222.
96 R. Cid and A. Lopez Agudo, *React. Kinet. Catal. Lett.*, 1983, **22**, 13.
97 D. G. Barton, S. L. Soled, G. D. Meitzer, G. A. Fuentes and E. Iglesia, *J. Catal.*, 1999, **181**, 57.
98 E. Iglesia, S. L. Soled and G. M. Kramer, *J. Catal.*, 1993, **144**, 230.
99 R. J. Pellet, *J. Catal.*, 1998, **177**, 40.
100 M. Santikunaporn, D. E. Resasco and W. E. Alvarez, (submitted for publication).
101 K. Foger and H. Jaeger, *J. Catal.*, 1989, **120**, 465.
102 K. Foger, *J. Catal.*, 1982, **78**, 406.
103 R. J. Fenoglio, G. M. Nuñez and D. E. Resasco, *J. Catal.*, 1990, **121**, 77.
104 D. Teschner, K. Matusek and Z. Paal, *J. Catal.*, 2000, **192**, 335.
105 G. Del Angel, B. Coq, R. Dutartre and F. Figueras, *J. Catal.*, 1984, **87**, 27.
106 F. J. Schepers, J. G. Van Senden, E. H. Van Broekhoven and V. Ponec, *J. Catal.*, 1985, **94**, 400.
107 R. J. Fenoglio, G. M. Nuñez and D. E. Resasco, *Appl. Catal. A: Gen.*, 1990, **63**, 319.
108 H. C. De Jongste, V. Ponec and F. G. Gault, *J. Catal.*, 1980, **63**, 395.
109 J. G. Van Senden, E. H. Van Broekhoven, J. Vreesman and V. Ponec, *J. Catal.*, 1984, **87**, 68.
110 H. Du, C. Fairbridge, H. Yang and Z. Ring, *Appl. Catal. A: Gen.*, 2005, **294**(1), 1.
111 U. Nylen, J. F. Delgado, S. Jaras and M. Boutonnet, *Appl. Catal. A: Gen.*, 2004, **262**(2), 189.